

Microdroplet-enabled co-cultivation and characterization of microbial communities

by

Ji Hyang Park

A dissertation submitted in partial fulfillment
of the requirements for the degree of
Doctor of Philosophy
(Chemical Engineering)
in The University of Michigan
2012

Doctoral Committee:

Assistant Professor Xiaoxia Lin, Co-Chair
Professor Mark A. Burns, Co-Chair
Professor Michael J. Solomon
Professor Vincent B. Young
Professor David H. Sherman

© Ji Hyang Park 2012

All Rights Reserved

For mom and dad

ACKNOWLEDGEMENTS

First, I would like to offer my sincerest thanks to my advisors, Professor Nina Lin and Mark A. Burns for their continuous support and guidance. Their enthusiasm to research deeply affected me and they became role models for me showing how a professional researcher should be. Whenever I was lost and experienced difficulties in my studies, they encouraged me immensely and guided me overcome the troubles. Moreover, I truly enjoyed the extensive research freedom and opportunities they have given to me. Their consistent and supportive aid enabled successful completion of my Ph.D. study.

I would like to express my gratitude to my committee members, Professor Michael J. Solomon, Vincent B. Young and David H. Sherman. When I have a meeting with them, I always obtained excellent and creative instructions. Professor Solomon gave many valuable suggestions and raises excellent questions at my preliminary exam and data meeting. I would like to say thank you to Professor Young and a research scientist in his lab, Judy Opp, for tremendous help in experiments cultivating and analyzing natural microbiota. He generously supplied mouse fecal samples as well as many valuable suggestions. Professor Sherman gave me a great insight into a tunicate microbiota and consistently sent fresh samples for us.

In addition, I would like to extend thanks to current and previous members of Burns group and Lin group. I would never finish my study without Brian Johnsons support. He gave tremendous assistance especially in the automated sorting project. Moreover, I want to say thanks to Burns group members, Kyung Eun, Minsoung,

Dustin, Fang, Sean, Ramsey, Eric, Irene, Jaesung, Steven and Lavinia. I have always enjoyed discussions with them and appreciated for sharing great lab and office experiences. It is my pleasure to acknowledge Lin group members, Marjan, Yu, Alissa, Jeremy, Mike and Fengming, all of whom are great people.

Finally, I want to thank my parents and brother in Korea. They have always trusted me and offered consistent support, which motivated all of my journey in my life. My beloved brother, Junghwan, started his own exploration while I was staying far from him. I wish him all the best in his life. His optimism, humor and energy have always affected me positively. Also, I am truly happy that I can dedicate my dissertation to my dad, having his 60th birthday in this year. I would like to say thank you to my mom, a great woman, who has cleverness I wish to have inherited. I am pleased to acknowledge all these support from my family.

TABLE OF CONTENTS

DEDICATION	ii
ACKNOWLEDGEMENTS	iii
LIST OF FIGURES	viii
ABSTRACT	x
CHAPTER	
I. Research Objective and Background	1
1.1 Microbial Communities in Nature	1
1.2 Microfluidic Approaches for Microbial Cultivation	4
1.3 Dissertation Overview	6
II. Microdroplet-Enabled Highly Parallel Co-Cultivation of Microbial Communities	8
2.1 Summary	8
2.2 Introduction	9
2.3 Results	10
2.3.1 Encapsulation of co-cultures in microfluidic droplets	10
2.3.2 Co-cultivation of a symbiotic pair	13
2.3.3 Co-cultivation of a triplet system	16
2.4 Discussion	20
2.5 Materials and Methods	22
2.5.1 Microfabrication	22
2.5.2 Construction of fluorescently-labeled synthetic symbiotic systems	23
2.5.3 Encapsulation of microbes	24
2.5.4 Cultivation and monitoring of microbes	24

III. Oxygen Gradient Construction for Co-Cultivation of Microbial Communities in Droplets	26
3.1 Summary	26
3.2 Introduction	27
3.3 Results and Discussion	29
3.3.1 Fabrication of a multi-layered microfluidic device	29
3.3.2 Construction of oxygen gradient	30
3.3.3 Cultivation of murine fecal microbiota	33
3.4 Materials and Methods	34
3.4.1 Fabrication of microfluidic devices	34
3.4.2 Droplet generation and retrieval	35
3.4.3 Oxygen gradient generation	36
3.4.4 Measurement of oxygen concentration using RTDP solution	37
3.4.5 Isolation and co-cultivation of murine fecal microbiota	37
3.4.6 Terminal restriction fragment length polymorphism	37
IV. Development of Microfluidic Devices for Automated Sorting of Droplets	39
4.1 Summary	39
4.2 Introduction	40
4.3 Results and Discussion	41
4.3.1 Handling a large number of droplets	41
4.3.2 Hydrodynamic droplet sorting based on bacterial growth	44
4.4 Materials and Methods	46
4.4.1 Connecting microcentrifuge tubes for incubation of a large number of droplets	46
4.4.2 Fabrication of microfluidic devices	47
4.4.3 Droplet generation	47
4.4.4 Droplet reinjection, spacing and sorting	48
4.4.5 Automated sorting of droplets with fluorescently labeled <i>E. coli</i>	49
V. Droplet-Enabled Co-Cultivation of Tunicate Microbial Communities	50
5.1 Summary	50
5.2 Introduction	51
5.3 Results and Discussion	53
5.3.1 Sequencing of 16S rDNA library from tunicate sample	53
5.3.2 Droplet-enabled co-cultivation of tunicate microbiota	55
5.3.3 Isolation of microbes from tunicates	59
5.4 Materials and Methods	61

5.4.1	Microfabrication	61
5.4.2	Isolation of microbial community from tunicates . .	61
5.4.3	Encapsulation, cultivation and monitoring of microbes	62
5.4.4	Retrieval of droplets after cultivation	63
5.4.5	16S rRNA library construction and sequencing . . .	63
5.4.6	Terminal restriction fragment length polymorphism (TRFLP)	64
VI. Concluding Remarks and Future Directions		65
6.1	Concluding remarks	65
6.1.1	Droplet-enabled co-cultivation of microbial commu- nities	65
6.1.2	Oxygen Gradient Construction for Co-Cultivation of Microbial Communities in Droplets	66
6.1.3	Automated sorting of droplets	67
6.2	Future directions	68
6.2.1	Co-cultivation of natural microbial communities un- der oxygen gradient	68
6.2.2	Application of automated droplet sorting	69
6.2.3	Further device development and investigation of mi- crobial communities	71
BIBLIOGRAPHY		74

LIST OF FIGURES

Figure

1.1	Types of microbial interactions	3
1.2	Diffusion-allowed cultivation of environmental samples.	3
1.3	Microfluidic approaches for microbial cultivation. (A) Array of microwells supporting microbial growth.	5
1.4	Microfluidic manipulation of droplets.	5
2.1	A microfluidic device for microbial co-cultivation.	11
2.2	Comparisons between experiments and calculations for cell distribution in droplets.	14
2.3	On-chip cultivation of a cross-feeding pair.	15
2.4	Comparison of a fast growing pair (K-12 W^- and Y^-) and a slow growing pair (EcNR1 W^- and Y^-) on the same device.	16
2.5	On-chip cultivation of a triplet system.	18
3.1	A microfluidic device for microbial co-cultivation.	30
3.2	Oxygen gradient established in a multi-layered microfluidic device.	32
3.3	Cultivation of murine fecal microbiota under oxygen gradient.	33
3.4	Construction of liquid channel outlets for droplet retrieval.	35
4.1	Device-centrifuge tube connection for increasing incubation throughput.	43
4.2	Automated droplet sorting.	45

4.3	Picture sequences captured from a video clip showing droplet sorting.	46
5.1	Picture of tunicate and molecular structure of ET-743.	52
5.2	Phylogenetic tree of 16S rRNA sequences.	54
5.3	Droplet-enabled co-cultivation of a tunicate microbial community in TSB and seawater.	55
5.4	TRFLP results of droplet-derived co-cultures.	57
5.5	Comparison between culture methods and culture media.	58
5.6	TRFLP results of tunicate samples collected from different seasons.	60
5.7	TRFLP results of tunicate microbiota prepared by different isolation methods.	62

ABSTRACT

Microdroplet-enabled co-cultivation and characterization of microbial communities

by

Ji Hyang Park

Co-Chairs: Xiaoxia Nina Lin and Mark A. Burns

The majority of existing microbial species, in particular bacteria living in synergistic communities, have not been cultured in the laboratory. One important reason behind this “unculturability” is that conventional laboratory cultivation is aimed at pure cultures of individual species. The objective of this dissertation is to develop microfluidic co-cultivation platforms to expand the repertoire of cultivable species from natural microbial communities and to characterize co-cultivated communities.

We first aimed to make use of highly parallel micro-droplets to co-cultivate symbiotic microbial communities. We fabricated a microfluidic device that could readily encapsulate and co-cultivate subsets of a community, using aqueous droplets dispersed in a continuous oil phase. To demonstrate the effectiveness of this approach in discovering synergistic interactions among microbes, we tested it with a synthetic model system consisting of cross-feeding *E. coli* mutants. This technology is being extended and applied to the investigation of drug-producing natural microbiota isolated from tunicates.

We next combined droplet co-cultivation with oxygen gradient generation to provide both the optimal oxygen concentration and the environment for microbial inter-

actions. Our device was composed of two glass layers with fluid channels separated by a 50- μm -thick PDMS membrane. A linear oxygen gradient established in the gas channel was successfully transferred to droplets in the liquid channel. A murine fecal microbial sample, of which the bacteria lived with limited oxygen concentration in their native environment, was cultivated and different species were enriched in chambers featuring different oxygen conditions.

To further parallelize and automate the droplet-enabled co-cultivation technology, we have also developed a simple and robust method for incubation of millions of droplets using a microcentrifuge tube, and have combined it with a microfluidic device for automated droplet sorting. Automated sorting is performed hydrodynamically based on analysis of fluorescent droplet images representing cell density after cultivation.

This dissertation demonstrates that droplet-enabled co-cultivation can effectively decompose complex microbial communities into subsets of symbiotic members and thus facilitate the elucidation of underlying microbial interactions. In addition, automated droplet sorting can be exploited for engineering purposes such as ultrahigh-throughput screening of microbial strain libraries.

CHAPTER I

Research Objective and Background

1.1 Microbial Communities in Nature

Our comprehension of microbial diversity has been explosively enhanced by culture-independent phylogenetic analysis of 16S rRNA sequences over the last few decades⁵⁶. The number of published microbial species now exceeds 10000 according to the taxonomy statistics of the National Center for Biotechnology Information⁹⁷, which is more than 500% increase compared to the number reported by 1980⁶¹. Furthermore, the total number of microbial species is roughly estimated⁵³ to reach 10^6 . Most of these natural microbes live in synergistic communities and the sequence-based approach has revealed the complexity of numerous microbial communities in nature since it was applied to microbial ecology studies in 1986⁸⁶. These microbial communities thrive in various environments and play important roles in a wide spectrum of ecosystems such as soil^{49,10,27}, ocean^{55,29} and other higher organisms as hosts^{25,110,111}. For example, various body sites of human are representative habitats for microbial communities and they massively affect human health in both positive and negative ways¹⁰⁶. Over 600 species have been isolated from human oral cavity and shown to cause diverse oral diseases³⁴. Human skin microbiota comprise more than 1000 species⁴⁶ and function in both of protection and infection²³. More importantly, human gut microbiota consisting of about 500 species have various roles related to human health includ-

ing nutrient digestion, development of immune system and repression of pathogenic microbial growth^{44,48,71,105}.

As our understanding of sequence-based microbial diversity and richness of microbial communities has been extended, the gap between the number of microbial species present in nature and that of cultivated species, so called as “great plate count anomaly” has been widened and received more attention. Less than 1% of microbial species has been isolated by conventional pure cultivation technique⁸³. For improvement of cultivation technology and explanation for why only a small fraction of microbial species is cultivable, significant efforts have been spent such as cultivation in media with low nutrient²⁴, mimicking of natural oligotrophic environment¹⁷, extension of culture time²⁸ and PCR-based surveillance method to screen the optimal culture conditions¹⁰¹. Among these approaches, representation of cell-to-cell signaling and interactions of natural microbiota has successfully isolated various species which had not been cultivated before^{17,15,36,66,84,39}.

Intercellular interactions in a natural microbial community are believed to be very important for maintenance of the community and survival of individual species. Many different kinds of interactions affecting populations have been found in natural microbial communities (Figure 1.1)²³. In particular, it has been reported that there exist various essential synergistic interactions between members of a microbial community depending on exchange of molecules and metabolites^{98,9,6}. Since conventional pure culture technique does not allow these cooperative interactions, the microbial species requiring such interactions for their survival cannot be isolated by pure cultivation.

To overcome the disadvantage of pure cultivation, researchers have tried to add various signaling molecules to cultures of environmental samples in synthetic media^{17,36,84}. However, targeting a specific molecule for promoting microbial growth is challenging because there exists not much information about essential microbial interactions for sustenance. Another approach to cultivate microbial species requir-

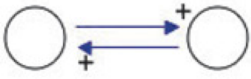

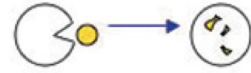
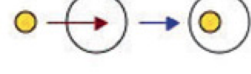


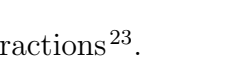
Connotation	Relationship	
Positive	Mutualism: Both species benefit and depend on each other for survival.	
	Protocooperation: Both species benefit but do not depend on each other for survival.	
	Commensalism: One species benefits while the other is unaffected.	
Negative	Predation: One species preys on another species.	
	Parasitism: One species benefits while the other is harmed.	
	Amensalism: One species kills another species.	
	Competition: One species out-competes the other for resources.	

Figure 1.1: Types of microbial interactions²³.

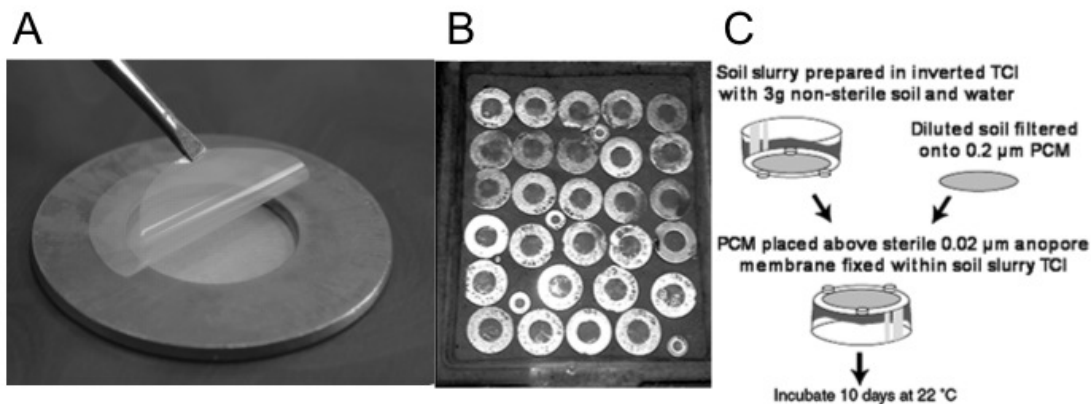


Figure 1.2: Diffusion-allowed cultivation of environmental samples. (A) A diffusion chamber allowing exchange of molecules during cultivation¹⁵. (B) An array of diffusion chambers isolating soli microbes⁶⁶. (C) Another design of cultivation on a membrane allowing molecular diffusion³⁹.

ing interactions is providing culture environment mimicking all microbial interactions present in the original habitat^{15,66,39}. In this type of cultivation, all secondary metabolites and signaling molecules are provided to isolated microbes by diffusion through a membrane (Figure 1.2). Although numerous new isolates were identified by this method, we cannot obtain any information about which interactions the new isolates relied on.

1.2 Microfluidic Approaches for Microbial Cultivation

Recent years have seen the increasing application of microfluidics, a powerful technological platform featuring small-scale and rapid operations, to cell cultivation and subsequent analysis. In particular, microfluidic compartmentalization has been widely utilized (Figure 1.3). For example, microwells have been used to confine and culture various microorganisms^{59,58}, including bacteria of which the growth was quorum-sensing dependent¹⁴. Microfluidically generated droplets represent another strategy for creating localized environments for diverse applications such as cell cultivation^{47,73,77,69}, screening²¹ and sorting¹². Compared to microwells, microdroplets are more easily subject to further manipulations such as splitting⁶⁵, merging¹⁶ and adding reagent¹ in microfluidic channels. It should be noted that microbial communities have started being examined using microfluidic approaches⁷³. Nevertheless, previous studies have focused exclusively on obtaining and analyzing pure cultures, which did not address the key question of how microbial interactions enable the sustenance of communities.

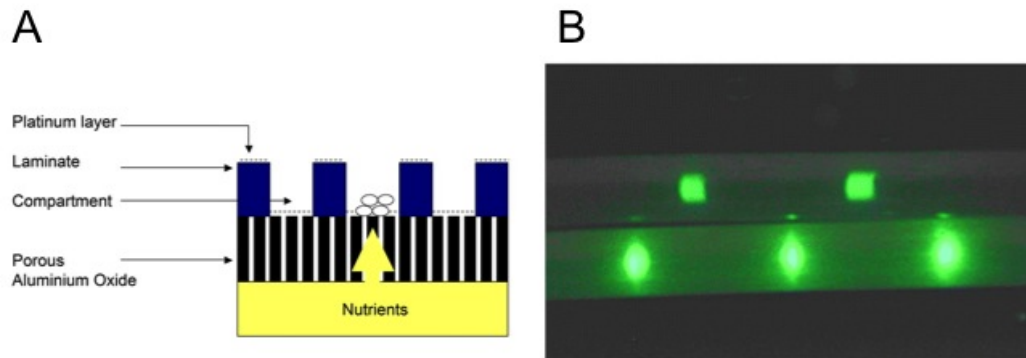


Figure 1.3: Microfluidic approaches for microbial cultivation. (A) Array of microwells supporting microbial growth⁵⁸. (B) Pure cultivation of fluorescently labeled *E. coli* in monodispersed droplets⁷⁷.

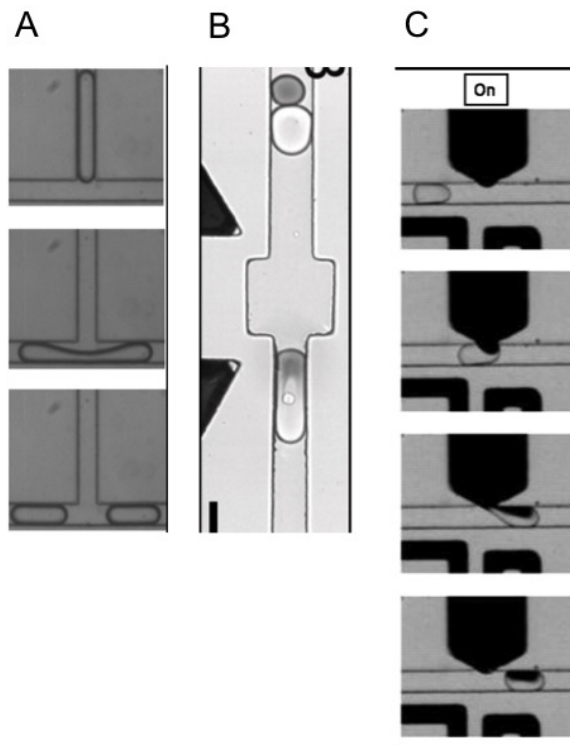


Figure 1.4: Microfluidic manipulation of droplets. (A) Breakup of a droplet at T-junction⁶⁵. (B) Fusion of droplets¹⁶. (C) Reagent injector for droplets¹.

1.3 Dissertation Overview

In order to expand the repertoire of cultivable species from natural microbial communities and to characterize co-cultivated communities, we first aimed to make use of highly parallel micro-droplets to co-cultivate symbiotic microbial communities and demonstrated its effectiveness in discovering synergistic interactions among microbes. We fabricated a microfluidic device that could readily encapsulate and co-cultivate subsets of a community, using aqueous droplets dispersed in a continuous oil phase. Microfluidically generated monodispersed droplets isolates various subsets from environmental samples allowing essential microbial interactions to be localized for survival of encapsulated members. To demonstrate the effectiveness of this approach in discovering synergistic interactions among microbes, we first tested it with a synthetic model system consisting of cross-feeding *E. coli* mutants. This platform was extended for the investigation of drug-producing natural microbiota isolated from tunicates.

We next combined the co-cultivation technology with oxygen gradient generation for providing both the optimal oxygen concentration and the environment for microbial interactions. Linear oxygen gradient established in the gas channel is successfully transferred to droplets in the liquid channel and the device has been applied to providing various oxygen levels in co-cultivation of a natural microbial community effectively.

For further parallelization and automation of the droplet-enabled technology, we finally developed a simple and robust device for incubation of millions of droplets using a microcentrifuge tube and combine it with a microfluidic device for automated sorting. Automated sorting was performed hydrodynamically based on the fluorescent image analysis of droplet images representing cell density after cultivation.

This dissertation shows that our droplet-enabled co-cultivation and its extension can effectively decompose complicated microbiota and thus facilitate the elucidation of underlying interactions. In addition, the automated technology can be utilized for

industrial purposes such as automated screening of engineered microbial strain from a library.

CHAPTER II

Microdroplet-Enabled Highly Parallel Co-Cultivation of Microbial Communities

2.1 Summary

Microbial interactions in natural microbiota are, in many cases, crucial for the sustenance of the communities, but the precise nature of these interactions remain largely unknown because of the inherent complexity and difficulties in laboratory cultivation. Conventional pure-culture-oriented cultivation does not account for these interactions mediated by small molecules, which severely limits its utility in cultivating and studying “unculturable” microorganisms from synergistic communities. In this study, we developed a simple microfluidic device for highly parallel co-cultivation of symbiotic microbial communities and demonstrated its effectiveness in discovering synergistic interactions among microbes. Using aqueous micro-droplets dispersed in a continuous oil phase, the device could readily encapsulate and co-cultivate subsets of a community. A large number of droplets, up to 1,400 in a 10mmx5mm chamber, were generated with a frequency of 500 droplets/sec. A synthetic model system consisting of cross-feeding *E.coli* mutants was used to mimic compositions of symbionts and other microbes in natural microbial communities. Our device was able to detect pair-wise symbiotic relationship when one partner accounted for as low as 1% of the

total population or each symbiont was about 3% of the artificial community.

2.2 Introduction

In nature, most microbes live in synergistic communities as a way to adapt to and thrive in various environments, such as the ocean^{103,30}, soil^{18,108}, and higher organisms as hosts^{51,54}. These microbial communities play important roles in a wide spectrum of ecosystems and form diverse interactions among community members and with their surroundings⁹⁸. For example, the human body is a representative host for natural microbial communities: over 100 trillion bacteria are estimated to be present in the human gut⁷⁶, more than 600 microbial species are known to inhabit the human oral cavity⁷⁵, and over 100 different bacterial 16S rRNA are present on human skin⁴⁵. These microbes are believed to be closely related to human health³³. For instance, the gut microbiota is known to contribute to digestion of nutrients⁴⁴, stimulation of immunity⁹² and protection of the host from inflammatory diseases⁷⁸. Despite their ubiquitousness and apparent significance, our understanding of these microbial communities remains very limited, largely owing to their inherent complexity and the difficulty in laboratory cultivation of most of the microbes.

The majority of existing microbial species, estimated to be in the millions, have not been cultured in the laboratory⁶⁶, which severely limits the extent to which they can be characterized and further studied. One important reason behind this “unculturability” is that conventional laboratory cultivation is aimed at pure cultures of individual species, while in nature, the survival and growth of microorganisms are largely associated with their interactions with other members of the community they live in^{98,66,31,13}. These interactions are mediated by various molecules such as secondary metabolites, quorum sensing molecules, and peptides^{43,112,102}. Accordingly, researchers have attempted to develop alternative cultivation techniques that allow interactions among microbes^{66,39,114,40,5}. For example, Kaeberlein et al. success-

fully isolated and cultured previously uncultivated marine microorganisms by using a multi-chamber set-up which allowed the diffusion of small molecules through membranes⁶⁶.

Recent years have seen the increasing application of microfluidics, a powerful technological platform featuring small-scale and rapid operations, to cell cultivation and subsequent analysis. In particular, microfluidic compartmentalization has been widely utilized. For example, microwells have been used to confine and culture various microorganisms^{59,58}, including bacteria of which the growth was quorum-sensing dependent¹⁴. Microfluidically generated droplets represent another strategy for creating localized environments for diverse applications such as cell cultivation^{47,73,77,69}, screening²¹ and sorting¹². It should be noted that microbial communities have started being examined using microfluidic approaches⁷³. Nevertheless, previous studies have focused exclusively on obtaining and analyzing pure cultures, which did not address the key question of how microbial interactions enable the sustenance of communities.

In this work, we aimed to make use of highly parallel micro-droplets to co-cultivate symbiotic microbial communities. We fabricated a microfluidic device that could readily encapsulate and co-cultivate subsets of a community, using aqueous droplets dispersed in a continuous oil phase. To demonstrate the effectiveness of this approach in discovering synergistic interactions among microbes, we tested it with a synthetic model system consisting of cross-feeding *E.coli* mutants, which can be used to mimic various compositions of natural microbial communities.

2.3 Results

2.3.1 Encapsulation of co-cultures in microfluidic droplets

Identification of symbiotic interactions among members in a microbial community can be facilitated by compartmentalizing and localizing the community for co-

cultivation. In this work, microfluidic devices were fabricated for encapsulating and co-cultivating subsets of a microbial community in monodispersed droplets. Encapsulated microbes can grow only if the droplet localizes symbiotic interactions in it (Figure 2.1A). The device comprised a slanted T-junction for droplet generation and a chamber to hold droplets for cultivation (Figure 2.1B,C). The slanted T-junction is able to generate monodispersed droplets with a single vacuum line at the outlet instead of multiple lines of pressure at the inlets. Increasing power of the vacuum led to increase of the frequency of droplet generation and subsequently the number of droplets in the chamber. The achievable range of frequency was 1-500 droplets/sec. When the frequency exceeded the maximum, the droplets were no longer monodispersed and co-flow of two immiscible phases occurred. The volume of droplets was largely determined by the channel geometry and was maintained at about 1nl in this work.

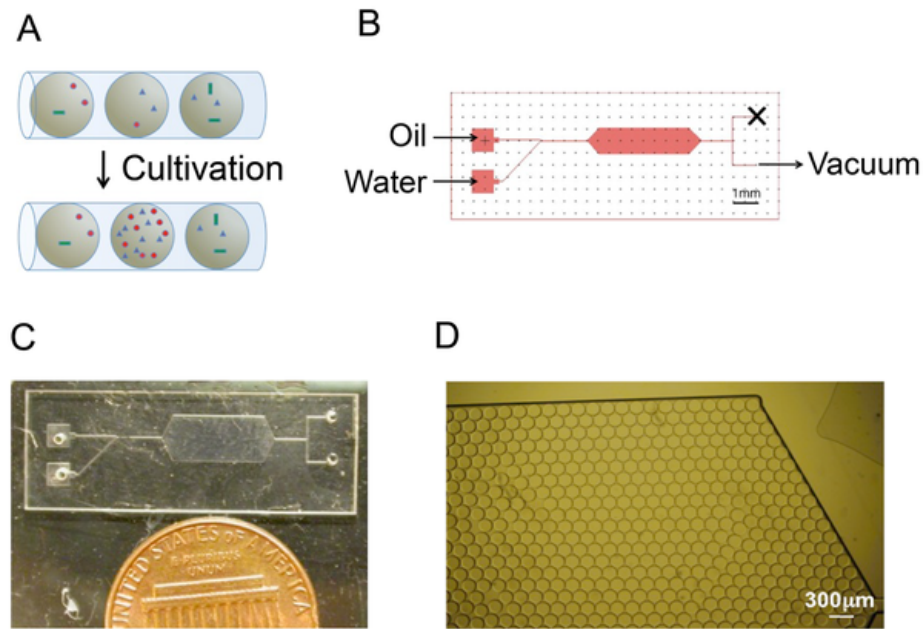


Figure 2.1: A microfluidic device for microbial co-cultivation. (A) Compartmentalized co-cultures enable detection of symbiotic relations among community members. (B) Schematic design of the microfluidic device. (C) A picture of the microfluidic device. (D) Droplets filling a large chamber in the microfluidic device.

Droplets generated from the T-junction were collected and held in the chamber for on-chip cultivation. Surfactant was dissolved in the oil phase⁵² and effectively stabilized the droplet surface. Up to 1,400 droplets could be packed very tightly in a 10 mm x 5 mm chamber (Figure 2.1D). After the droplets filled the chamber, the vacuum was removed and the flow stopped immediately. Droplets could be stably incubated for 4 days.

We hypothesized that compartmentalization of different microbial species in a community are independent events and for each species, the number of encapsulated cells in a droplet follows the Poisson distribution. For experimental validation of this hypothesis, a co-culture consisting of two differently labeled *E. coli* strains, named W^- and Y^- , was injected into the device and the distribution of cells was examined with fluorescence microscopy. As shown in Figure 2.2A, for each strain, the experimentally measured distribution of droplets carrying various numbers of cells agreed very well with calculated values using the Poisson distribution. The average number of cells in each droplet, which corresponded to the λ parameter in the Poisson distribution, was dependent upon the cell density in the seed culture injected into the device and the droplet volume determined by the device configuration.

As each species' distribution in droplets is expected to follow a simple Poisson distribution and different species are encapsulated independently, we could readily predict the distribution of the four combinations (i.e. $W^- Y^-$, W^- only, Y^- only, and empty). Not surprisingly, there was a very good agreement between the calculated values and measured ones (Figure 2.2B). This experimental validation was successfully extended to the distribution of a triplet system when a third strain, S^- , was added (Figure 2.2C). Therefore, the distribution of encapsulated subsets of a microbial community is highly predictable given the total cell concentration and composition of the community. Accordingly, for a given community composition, it is possible to determine the optimal cell density of the seed culture for a fixed device

to achieve a desired droplet distribution.

2.3.2 Co-cultivation of a symbiotic pair

To mimic natural communities of interacting microbes, a synthetic symbiotic *E.coli* system consisting of a tryptophan auxotroph and a tyrosine auxotroph was constructed. Each auxotroph is unable to synthesize the corresponding amino acid and hence cannot survive in minimal media. However, when both auxotrophs are present, they can grow in the minimal medium by cross-feeding (Figure 2.3A). To monitor the co-culture composition, each strain was labeled with a fluorescent protein and counted by microscopy.

On-chip co-cultivation of the tryptophan auxotroph (abbreviated to W^-) and the tyrosine auxotroph (abbreviated to Y^-) demonstrated that droplets could effectively compartmentalize co-cultures of microbes. Seed cultures of W^- and Y^- were diluted with the minimal medium and mixed properly such that the $W^-:Y^-$ ratio was 1 : 1 and upon injection into the device, the average cell number per droplet was about 0.6. A total of 608 droplets were generated in this experiment. Of those, 317 were empty. 83 and 150 droplets had W^- only and Y^- only, respectively. 58 consisted of the W^- and Y^- pair.

After 18 hours of cultivation, only the cells in the droplets carrying both W^- and Y^- cells were growing well (Figure 2.3B,C). We noted that some of the droplets carrying W^- or Y^- only were adjacent to droplets carrying the W^- and Y^- pair during cultivation, but cells in these droplets did not grow. This implied that the diffusion of amino acids did not occur across the droplet boundaries. In other words, the oil-water interface effectively blocked molecular diffusion between different droplets and therefore the droplets could generate highly parallelized and localized co-cultivation environments for detecting symbiotic relationships in a large and complex microbial community.

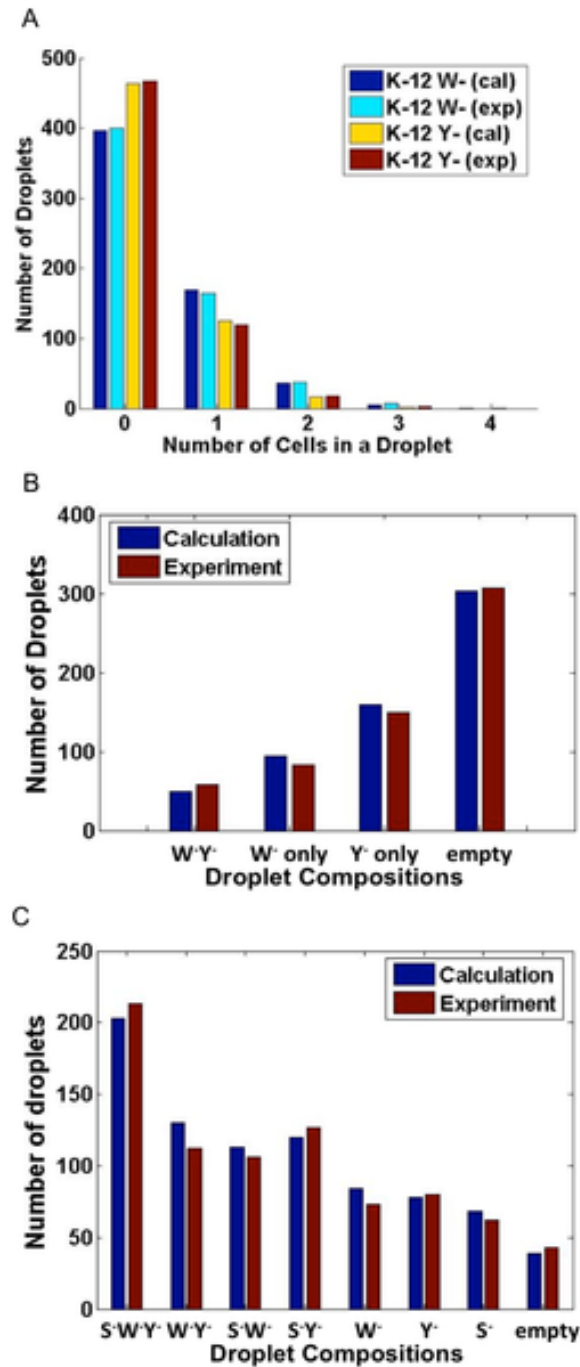


Figure 2.2: Comparisons between experiments and calculations for cell distribution in droplets. Calculations were based on the Poisson distribution. (A) Numbers of droplets carrying different numbers of cells. (B) Numbers of droplets carrying four different combinations of a two-strain system. (C) Numbers of droplets carrying eight different combinations of a three-strain system.

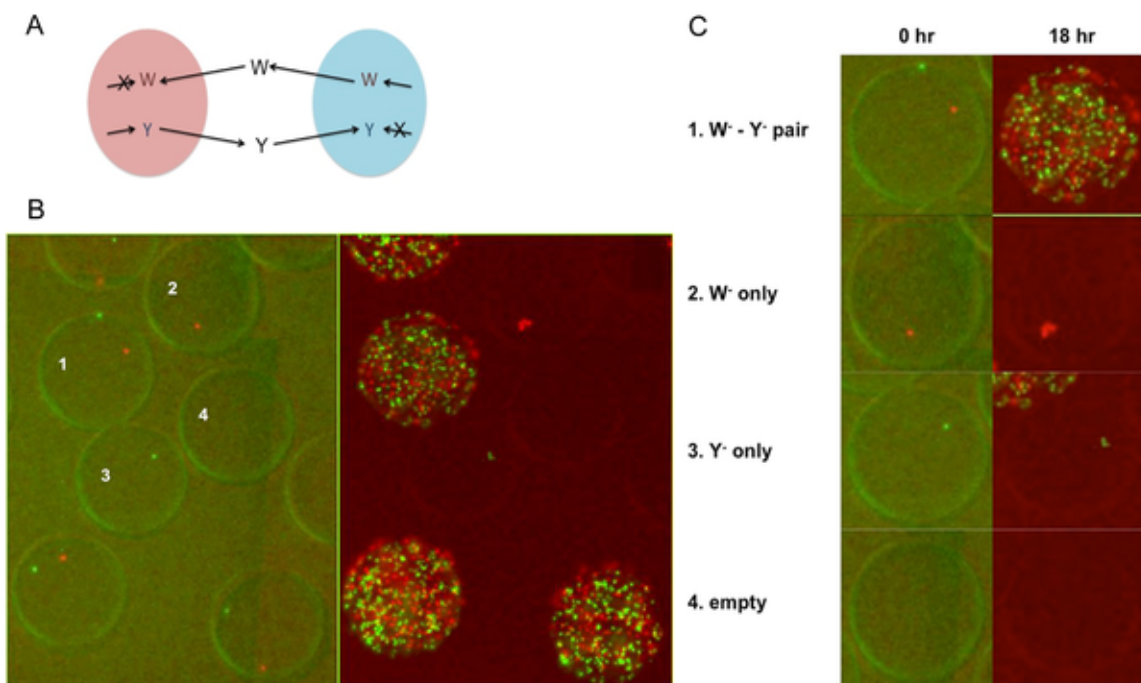


Figure 2.3: On-chip cultivation of a cross-feeding pair. (A) A synthetic symbiotic system consisting of two cross-feeding amino acid auxotrophs. (B) A section of the large cultivation chamber illustrating a number of droplets carrying four combinations of the two-strain system. *E. coli* strain Y^- is labeled with yellow fluorescence (EYFP) and W^- with red fluorescence (mCherry). Left - before cultivation, Right - Pictures after 18-hour cultivation. (C) Comparison of four individual droplets from Panel (B).

On-chip droplet-based co-cultivation could further distinguish stronger symbiotic relationships from weaker ones among subsets of microbes. This could be demonstrated by examining two different strains of the tryptophan auxotroph when they were paired with the tyrosine auxotroph. We made use of a K-12 W^- strain and an EcNR W^- strain. Both grew with *E. coli* K-12 Y^- in the minimal medium, while the K-12 W^- and Y^- pair co-grew 50% faster than the EcNR W^- and Y^- pair in macro-scale tube cultures (growth rates: $0.189 - 0.011 \text{ hr}^{-1}$ versus $0.126 - 0.004 \text{ hr}^{-1}$). As shown in Figure 2.4, when we injected a mixed culture of K-12 W^- , EcNR W^- , and Y^- with a ratio of 1 : 1 : 10 into the device, cells in droplets containing K-12 W^- and Y^- (Figure 2.4A) grew significantly better than those in droplets containing EcNR

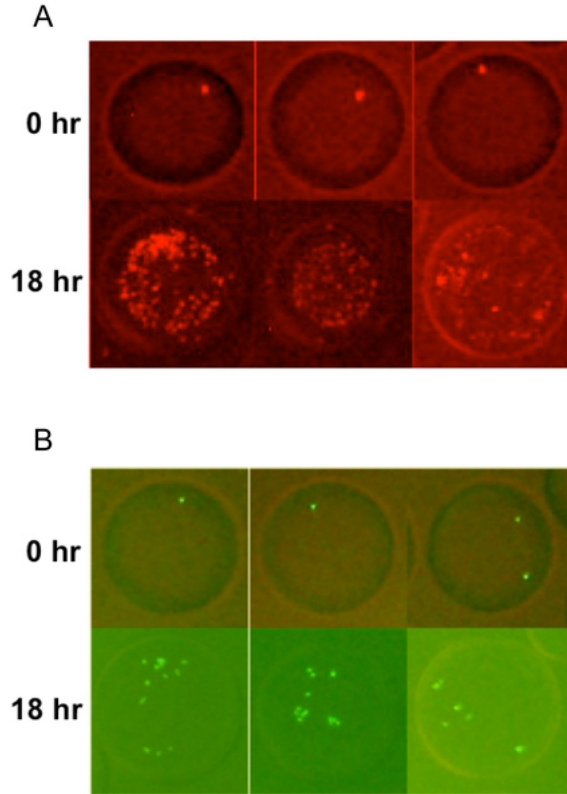


Figure 2.4: Comparison of a fast growing pair (K-12 W^- and Y^-) and a slow growing pair (EcNR1 W^- and Y^-) on the same device. (A) Three droplets carrying the pair of *E.coli* K-12 W^- expressing mCherry and Y^- (not labeled with fluorescence). Top panels - before cultivation. Bottom panels - after 18-hour cultivation. (B) Three droplets carrying the pair of *E.coli* EcNR1 W^- expressing GFP and K-12 Y^- . Top panels - before cultivation. Bottom panels - after 18-hour cultivation.

W^- and Y^- (Figure 2.4B).

2.3.3 Co-cultivation of a triplet system

To mimic the complexity of natural communities more realistically, we introduced a third amino acid auxotroph, a serine auxotroph, into the system (Figure 2.5A). The serine auxotroph (abbreviated to S^-) was previously found to form no cross-feeding relationship with W^- or Y^- and hence could be considered as the background or noise in the community. We first examined the simplest case where the ratio of $S^- : W^- : Y^-$ was 1 : 1 : 1. The average number of cells in each droplet was controlled

to be three. For counting of cells and monitoring of growth, S^- , W^- and Y^- were labeled with CFP, mCherry and EYFP, respectively. In this triplet system, eight different combinations were possible. A total of 816 droplets were generated and the number of droplets carrying each combination is shown in Table 1. As expected, among these droplets, only the cells in the droplets carrying the W^- and Y^- pair or the S^- , W^- and Y^- triplet were able to grow, as shown in Table 2.1 and Figure 2.5. In particular, 112 droplets carried W^- and Y^- initially and 109 of them (97%) supported growth very well after 18 hours. This result showed that the droplet device was able to detect symbiotic relationships among subsets of members despite the presence of other microbes in the community.

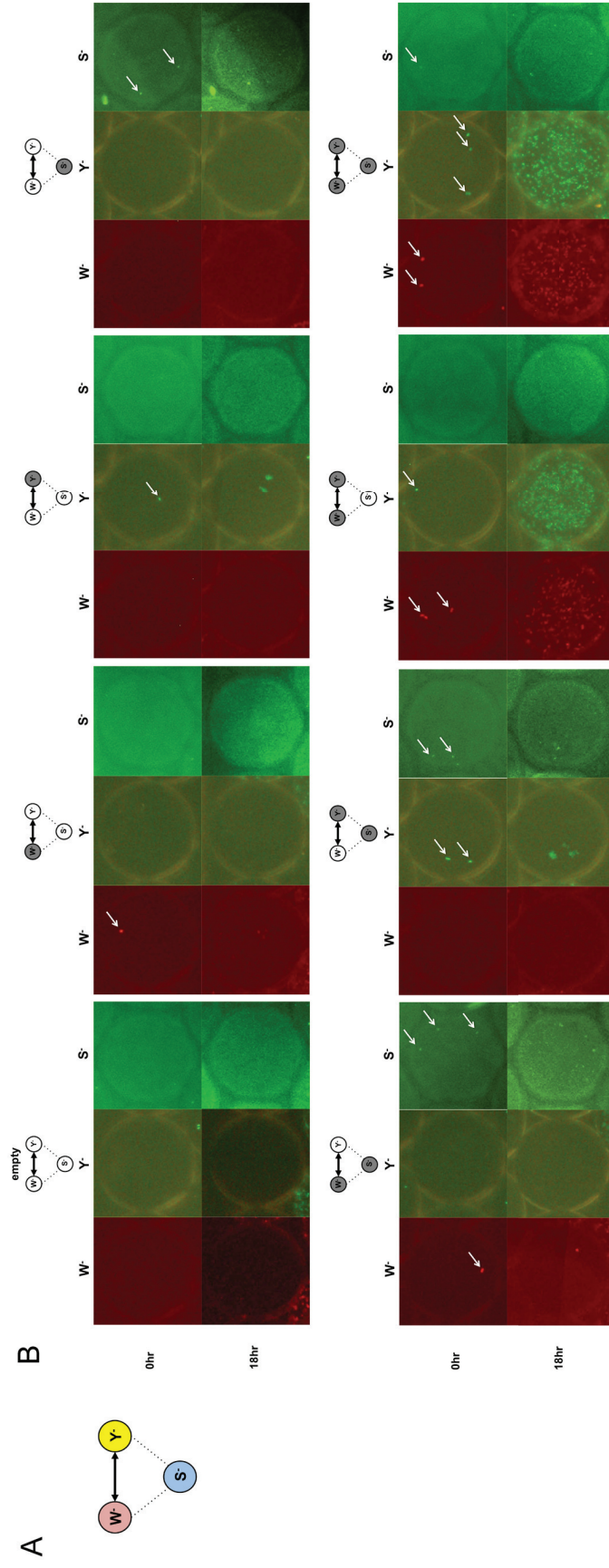


Figure 2.5: On-chip cultivation of a triplet system. (A) A synthetic system of three amino acid auxotrophs (W^- , Y^- , and S^-). Only W^- and Y^- forms a symbiotic relationship. (B) Eight droplets illustrating all the combinations of the triplet system. Top panels are pictures taken before the cultivation and bottom panels are at 18 hours.

In natural microbial communities, symbiotic partners might account for a small fraction of the total population. To mimic such conditions in nature, we further examined two other compositions of the *E. coli* triplet system. In one scenario, one partner of the symbiotic pair is a rare species; in the other, both partners are rare. In both cases, we tested the limit to which the device was able to detect the symbiosis between W^- and Y^- by generating droplets containing both and hence supporting co-growth of the pair. For the first case, we examined a mixed culture with the ratio of $S^- : W^- : Y^- = 50 : 50 : 1$, in which Y^- is a rare species accounting for about 1% of the total population. Based on simulation of cell distribution in droplets, we selected the average number of cells in each droplet to be five. To generate this average cell number per droplet, we estimated the density of the mixed culture under microscope using a Petroff-Hausser counting chamber and then diluted accordingly before injecting it into the device. Using a device with a 3mmx10mm incubation chamber, we generated a total of 880 droplets. As shown in Table 2.1b, because of the dominance of S^- and W^- in the population, the majority of the droplets contain either one or both of them, without the presence of the rare Y^- . Nevertheless, four droplets turned out to contain the W^-/Y^- pair, eighteen droplets encapsulated all three strains, and most of them (19 out of 22) showed well-sustained co-growth. It should be noted that for our synthetic system, the W^-/Y^- pair can co-grow when S^- is present and hence the above two types of droplets (i.e. W^-/Y^- and $S^-/W^-/Y^-$) can both detect the existing symbiotic relationship. However, in natural microbial communities, due to negative interactions with other species⁴⁸, symbiotic partners may not be able to grow when other species are present. In this case, only the droplets that contain the symbiotic partners (e.g. W^-/Y^- in our model system) are desirable for supporting co-cultivation and detection of symbiotic relationships.

In the second case, we focused on the ratio of $S^- : W^- : Y^- = 30 : 1 : 1$, which exemplified symbiotic relationships existing between two rare species (here,

each partner is about 3% of the total population). We chose to encapsulate an average of three cells in each droplet and generated a total of 977 droplets on a device with a 3mmx10mm chamber. In this scenario, a large fraction of the droplets contain S^- , as detailed in Table 2.1 C. Nevertheless, we managed to observe six droplets that encapsulated the W^-/Y^- pair, including one containing only these two strains. All of these droplets supported the co-growth of W^-/Y^- very well. The above results demonstrated that our device and co-cultivation method can effectively capture and amplify rare species in a microbial community and detect their symbiotic relationships with either abundant or other rare species.

(A)

	empty	S^-	W^-	Y^-	S^-W^-	S^-Y^-	W^-Y^-	$S^-W^-Y^-$
Growth	0	0	0	0	0	0	109	210
No Growth	43	62	73	80	106	127	3	3

(B)

	empty	S^-	W^-	Y^-	S^-W^-	S^-Y^-	W^-Y^-	$S^-W^-Y^-$
Growth	0	0	0	0	0	0	3	16
No Growth	40	153	138	2	515	6	1	2

(C)

	empty	S^-	W^-	Y^-	S^-W^-	S^-Y^-	W^-Y^-	$S^-W^-Y^-$
Growth	0	0	0	0	0	0	1	5
No Growth	32	798	2	1	78	70	0	0

Table 2.1: Number of droplets carrying various subsets of the triplet system.

(A) $S^-:W^-:Y^- = 1:1:1$ (B) $S^-:W^-:Y^- = 50:50:1$ (C) $S^-:W^-:Y^- = 30:1:1$.

2.4 Discussion

In this work, we have demonstrated that microfluidically generated droplets can be effectively utilized to co-cultivate microbes and detect symbiotic relationships. Two features of our microfluidic device contributed to this effectiveness. First, due to its small dimensions and rapid operation, our droplets based device can achieve compartmentalization of microbial communities in a highly parallel and automated manner. Second, the interface between the aqueous phase in the droplet and the

oil phase prevents molecular exchanges, and hence the cultivation environment in individual droplets is completely localized.

We used a synthetic *E.coli* symbiotic co-culture as a model system in this proof-of-concept study. Nevertheless, the platform we presented here for on-chip co-cultivation can be readily applied to a wide range of natural microbial communities. As shown in this work, the distribution of cells in droplets is highly predictable. Therefore, for a given microbial community with certain total density and composition, the design (e.g. droplet and chamber size) and operation (e.g. dilution ratio) of our microfluidic device can be optimized to co-cultivate and examine community members at different levels of abundance. For example, in this work, with up to 1,000 droplets, we could adjust the dilution ratio to detect the synthetic symbiotic interaction when one or both of the pair was very rare in the population. In addition, we showed that different extent of symbiosis could also be distinguished. Thus, our work suggests a promising new approach for cultivating microbes and for understanding microbial interactions. We can use this approach to cultivate and isolate various microbes of which the growth requires support (e.g. through signaling) from other species in the community. The cell cultures can then be further studied using a variety of characterization and analysis methods such as (meta)genome sequencing. Moreover, the co-growth data obtained from this co-cultivation approach will reveal positive relationships among community members, such as those between *Bifidobacterium adolescentis* and butyrate-producing anaerobes in the human gut¹³, and negative ones. Elucidation of these microbes and their interactions might have important implications for many applications such as diagnostics and treatment of polymicrobial diseases.

This work represents an initial step towards the elucidation of microbe-microbe-environment interactions of complex communities based on microdroplet co-cultivation and characterization. To fulfill this long-term goal and to apply this approach to real

microbial communities, we have identified two key tasks that require further efforts. First, automated droplet sorting and retrieval will enable us to distinguish droplets with well-developed mixed cultures from those with little growth and to obtain each of them individually. This can be achieved by coupling microscopy with flow control of droplets³. Second, when studying natural microbial communities, in which none of the cells is labelled, we need to characterize the retrieved droplet-mediated mixed cultures. Three genetic approaches with varying levels of details are suitable for this purpose. Terminal restriction fragment length polymorphism (T-RFLP) of 16s rDNA is a simple method that can rapidly determine how many species are present in the cultivated communities⁷⁴. Sequencing of 16s rRNA will identify the cultured microbes at a species level. Finally, whole genome amplification followed by metagenome sequencing will potentially lead to comprehensive and detailed understanding of the genetic basis underlying the microbial interactions^{67,107}. We are currently investigating these microfluidic developments and off-chip characterization methods, which will facilitate the scale-up of the approach presented in this work for application to complex natural microbial communities.

2.5 Materials and Methods

2.5.1 Microfabrication

We used glass devices. Channels were fabricated using general photolithography processes. A glass wafer was prepared with Cr-Au deposition and AZ1518 spin coating. The pattern of the Cr mask was transferred to the AZ1518-coated glass wafer with the UV exposure of LI 300 for 30 seconds. After developing for 1 minute in MF319 developer, Au and Cr were etched for 2 minutes. The glass wafer was wet-etched by HF, until the depth of the channel reach 50 μm . The channel depth was measured periodically by depth profiler during the etching process. After dicing the

individual devices, holes for inlets and outlets were electrochemically drilled in sodium hydroxide solution. To make the surface hydrophobic, a 2 μm -thick Parylene film was deposited on the channel and a cover slip. Afterwards, the channel and the cover slip were bonded with UV glue. Glass tubes were attached with UV glue at the holes as reservoirs of inlets and outlets, and syringe tips were fixed to the oil inlet and outlet reservoirs with epoxy to connect the device to vacuum source and oil reservoirs. Before using the devices for the cultivation, all devices were exposed to UV for at least one hour for sterilization. All devices were regenerated after each use. They were heated in a 540 °C furnace for 2 hours, followed by cleaning in Piranha solution of $\text{H}_2\text{O}_2:\text{H}_2\text{SO}_4 = 1:2$. Parylene coating, bonding with UV glue, attaching reservoirs and sterilization were repeated as described above.

2.5.2 Construction of fluorescently-labeled synthetic symbiotic systems

Four *E.coli* strains were used in this work and all were amino acid auxotrophs constructed through the deletion of genes or operons encoding key enzymes in the amino acid biosynthesis pathways. K-12 W^- , K-12 Y^- , and K-12 S^- were constructed by deleting *trpE*, *tyrA*, and *serA*, respectively, in *E.coli* K-12. In addition, *tyrR* was deleted in K-12 W^- to increase the co-culture fitness when it is paired with K-12 Y^- . All of the above gene deletions were carried out via P1 transduction with single-gene knock-out *E.coli* mutants from the Keio collection. After the transduction, the selection marker (*kan* gene) was deleted by transformation with the plasmid PCP20. The EcNR W^- strain was previously constructed by recombinogenic substitution of the *trpLEDCBA* operon with a selection marker (*cat* gene) in a derivative strain of *E.coli* MG1655 harboring a λ Red prophage. This tryptophan auxotroph strain grew at a slower rate when paired with K-12 Y^- .

For labeling of different strains, four fluorescent proteins, mCherry, EYFP, CFP, and GFP, were utilized. mCherry and GFP were inserted into pET24b and EYFP

into pET17b plasmids, respectively. The PBAD promoter was inserted in front of the fluorescent gene, deleting the original T7 promoter and lac operator. Resulted plasmids were transformed into different strains as needed. CFP was integrated into the chromosome at the galk locus via P1 transduction with RP22³⁷ as the donor strain.

To prepare seed cultures for on-chip cultivation, cells expressing mCherry, GFP and EYFP were cultivated overnight in LB media containing 0.4% arabinose and cells labeled with CFP in LB media containing 0.2 mM IPTG. Then each strain was harvested and diluted 100 times in M9 minimal medium containing 0.4% arabinose and 0.2 mM IPTG. After the cell density of each seed culture was estimated using a Petroff-Hausser counting chamber and a fluorescence microscope, the diluted seed cultures were mixed to obtain the desired ratios.

2.5.3 Encapsulation of microbes

A PFPE-PEG block copolymer surfactant⁵² (RainDance Technologies) was dissolved in fluorinated oil HFE-7500 (3M) at a final concentration of 2% wt/wt. The oil phase was supplied in a syringe connected to the device. After the device was connected to the vacuum source, 30 μ l of diluted cell mixture was added into the aqueous-phase inlet reservoir. Using LabView interface, continuous vacuum was turned on, and the power of the vacuum was increased gradually to 150-300 mmHg. After enough droplets were generated, vacuum was turned off. All syringes and connections were removed from the device. 5 μ l of mineral oil was added to each reservoir to prevent the evaporation of fluorinated oil.

2.5.4 Cultivation and monitoring of microbes

As soon as droplet generation was completed, the device was examined by microscopy. Pictures at the beginning and the end of cultivation were taken by Olympus

BX-51 and DP-71 with 20x objective lens. Exposure time and ISO were 0.25 sec/800, 0.8 sec/1600, and 0.2 sec/400 for mCherry, EYFP and CFP, respectively. For all pictures of CFP-expressing cells, autolevel and autocolor functions in Adobe Photoshop were applied to enhance the contrast. ImageJ was used to combine pictures from different channels. The device was placed in an incubator of 37 °C for cultivation and pictures were taken as needed.

CHAPTER III

Oxygen Gradient Construction for Co-Cultivation of Microbial Communities in Droplets

3.1 Summary

The natural habitats of microbial communities provide the best environment for their proliferation, including the interactions between neighboring microbes and the optimal oxygen concentration. Oxygen is toxic to some microbes, and oxygen tolerance and preference of microbes are different species by species^{57,96}. Providing oxygen concentration that mimic their natural environment, therefore, can greatly enhance the likelihood of cultivating diverse species from a community. Previously, we developed a microfluidic device for highly parallel co-cultivation of symbiotic microbial communities in droplets and demonstrated its effectiveness in discovering synergistic interactions among microbes⁸⁹. Extending this technology, here we have developed a multi-layered device for co-cultivation of microbes in droplets under a gradient of oxygen concentration ranging from 0% to 21% of oxygen. Our device is composed of two glass layers with fluid channels separated by a 50- μm -thick PDMS membrane. Oxygen gradient is established and maintained via a tree-shaped channel mixing humidified nitrogen and air flows, which is then transferred through the porous PDMS membrane to the chambers in the liquid channel incubating droplets. The linear

gradient was verified by measuring the fluorescence of 2mg/mL RTDP in droplets. A murine fecal microbiota, which lived with limited oxygen concentration in their original environment, was cultivated and different species were enriched in chambers featuring different oxygen conditions. Combined with the localization of symbiotic microbes in droplets, establishment of oxygen conditions mimicking their natural habitats can expand the repertoire of cultivable microbes, and thus, facilitate the elucidation of microbial interactions in a community.

3.2 Introduction

Oxygen tolerance and preference of bacteria are different from one species to another. While aerobic bacteria require oxygen to produce energy, obligate anaerobes cannot survive in presence of oxygen because of their lack of enzymes to process toxic byproducts of oxygen reduction such as peroxide, superoxide and oxygen radicals⁹⁶. There is a wide spectrum of bacteria, based on their ability of respiration, fermentation and removal of toxic oxygen molecules, ranging from aerobes, facultative aerobes, microaerobes, to aerotolerant anaerobes and obligate anaerobes. As a result, microorganisms require the optimal level of oxygen to thrive.

The natural habitats of microbial communities provide the best environment for their proliferation, including the optimal oxygen concentration and the interactions between neighboring microbes. For example, a vast range of microbial species such as strict anaerobes, facultative anaerobes⁵⁰ and microaerobes⁶⁴ colonize the gastrointestinal tract of a mammalian host. The abundance of individual species varies according to environmental changes such as surgical operation⁵⁰ and immune deficiency of the host⁸². In particular, microaerophiles isolated from human stomachs, *Campylobacter* and *Helicobacter*, have received intensive research attention because of their pathogenicity⁴¹. Providing the optimal oxygen concentration in cultivation, therefore, is required to enrich the bacteria of interest which have specific levels of

oxygen tolerance and preference. However, exploring various oxygen levels for optimization of conventional cultivation is very challenging and time-consuming due to the requirement of cylinders with distinct gas compositions and airtight chambers insulated from the atmospheric environment.

Microfluidic platforms can be used to provide various oxygen levels during cell cultivation. Flow in a microfluidic channel is laminar, so that the streamlines are maintained. Appropriate fluid-mixing geometry can be used to generate a variety of gradients of diffusible solutes. Many different designs for mixing have been developed^{60,7} and one representative channel design is a tree-shaped mixing geometry⁶³. In this geometry, various gradients of solute can be established by changing channel geometry³² and flow rates⁷². These gradient-generating technologies have been applied for various biological purposes such as investigation of bacterial chemotaxis³⁸, cancer metastasis, and immune responses⁶⁸. Researchers have also developed microfluidic devices to construct oxygen gradients in microfluidic channels^{2,20,100}. All of them were used for cell cultures in a single phase device^{20,100,70}.

We previously developed a microfluidic device for droplet-enabled co-cultivation of microbial communities to investigate microbial interactions, by encapsulating subsets of a microbial community⁸⁹. Monodispersed microdroplets provided a well-localized environment in a highly parallelized manner and enabled the detection of symbiotic relationships between members of a microbial community. In this work, we aim to combine the co-cultivation technology with oxygen gradient generation to expand the repertoire of cultivable species by providing both the optimal oxygen concentration and the environment for microbial interactions. A multi-layered device has been designed and fabricated, which consists of two glass layers with fluid channels separated by a 50 μ m-thick PDMS membrane. Oxygen gradient established in the gas channel is successfully transferred to droplets in the liquid channel and the device has been applied to providing various oxygen levels in co-cultivation of a natural microbial

community effectively.

3.3 Results and Discussion

3.3.1 Fabrication of a multi-layered microfluidic device

Droplet-enabled localized co-cultivation of a microbial community under various oxygen concentrations is achieved using a multi-layered microfluidic device (Figure 3.1 A,B). It is composed of two glass layers with fluid channels separated by a 50- μm gas-permeable PDMS membrane (Figure 3.1C). A gas channel generates gradient of oxygen concentration by mixing laminar flows of pure nitrogen and compressed air, and the gradient is transferred to droplets in the liquid channel through the PDMS membrane. Reynolds number of gas flow in microfluidic channel can be calculated as below:

$$Re = \frac{vL}{\nu}$$

where v is linear velocity, L is characteristic length, and ν is kinematic viscosity of fluid. For a rectangular channel, L is defined as $4A/P$, where A is the cross-sectional area and P is the wetted perimeter. Volumetric flow rate of gas ranges from 2 ml/hr to 5 ml/hr, A is $7.5 \times 10^{-9} \text{ m}^2$ and v varies from $7.41 \times 10^{-2} \text{ m/s}$ to $1.85 \times 10^{-1} \text{ m/s}$. Since ν of air at 37 °C is $15.68 \times 10^{-6} \text{ m}^2/\text{s}$ and L is $7.5 \times 10^{-5} \text{ m}$, Re ranges from 0.35 to 0.89. Two gas flows in laminar regime are mixed in gas channels and consequently, generate oxygen gradient.

Although the PDMS membrane is thin and highly permeable to gases, PDMS is permeable to oxygen almost twice as much as to nitrogen; permeability of PDMS to oxygen and nitrogen is $2.7 \times 10^{-13} \text{ mol m}/(\text{m}^2 \text{ sPa})$ and $1.37 \times 10^{-13} \text{ mol m}/(\text{m}^2 \text{ sPa})$, respectively⁸⁰. With bare PDMS membrane, the oxygenic environment in liquid chambers would be more oxygen-rich than expected. However, a 2 μm -thick hydrophobic Parylene coating on the liquid channel is required to create aqueous droplets dispersed

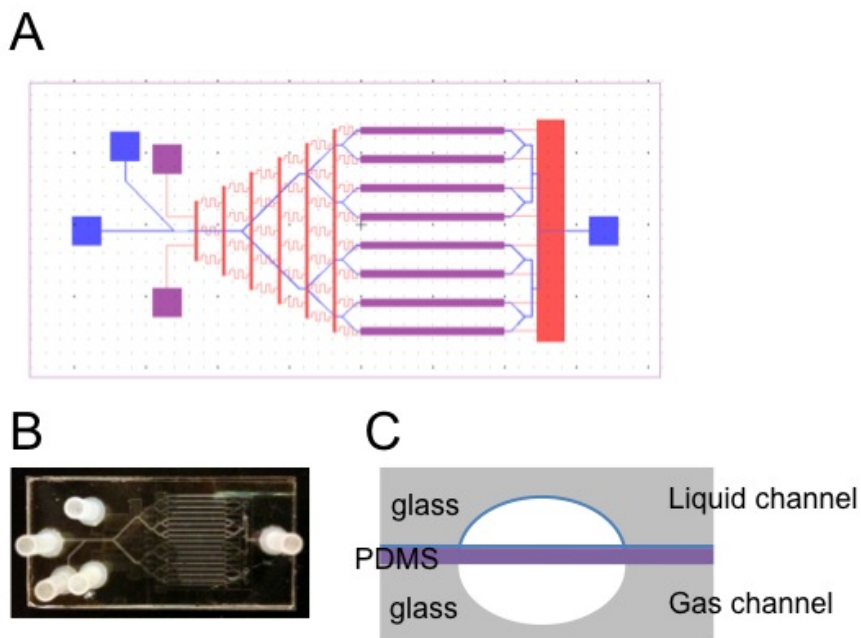


Figure 3.1: A microfluidic device for oxygen gradient construction. (A) Design of the microfluidic device. Blue and red channels represent liquid and gas channels, respectively. (B) Picture of the device. (C) A cross-sectional view of the device.

in oil and its very low gas permeability¹¹³ becomes the bottleneck for gas diffusion. The linear oxygen gradient could be transferred to the liquid channel.

3.3.2 Construction of oxygen gradient

For generation of linear oxygen gradient, two gas flows are connected to the inlets of the gas phase channel (Figure 3.2A). Before connecting the gas flows, all inlets and outlets of the liquid channel are sealed with epoxy after droplet generation. The low rate of the gases are controlled by pressure regulators installed at gas cylinders and maintained at 2ml/hr. The gases from both cylinders are extremely dry and droplets in the liquid channel would start to shrink due to evaporation within 6 hours. In order to prevent the evaporation, humidification bottles half-filled with DI water are inserted between pressure regulators and gas inlets of the device. With the humidification bottles installed, the device could stably incubate droplets for at least

48 hours.

To demonstrate that the gas phase can penetrate Parylene-coated PDMS membrane, the oxygen concentration of droplets were monitored in real time when the gas flow was changed from pure nitrogen to oxygen. Oxygen concentration measurement was performed using ruthenium tris(2,2'-dipyridyl) dichloride hydrate (RTDP) (Figure 3.2B). Because the fluorescent signal of RTDP molecules is quenched by oxygen molecules dissolved in a solution, measuring the fluorescent signal of RTDP droplets enables us to monitor the change of oxygen concentration of droplets in real time⁷⁹. Stage of a microscope was fixed and the fluorescent signal of the fixed region was recorded by a photodiode and a lock-in amplifier every second. RTDP droplets were initially equilibrated with atmospheric condition (21% of oxygen). The fluorescent signal was observed to increased with pure nitrogen flow and decreased with pure oxygen flow (Figure 3.2C). In addition, as expected, the change in fluorescence with pure nitrogen flow was much smaller than the change with pure oxygen flow. It took about two hours to reach a new equilibrium due to Parylene film, nevertheless, the gas beneath the PDMS membrane was transferred effectively to the droplets in the liquid channel.

A linear gradient of oxygen concentration was established by connecting nitrogen and compressed air to the gas inlets of the device. The average and standard deviation of fluorescent signals of fifteen droplets from each chamber are shown in Figure 3.2 D. Four conditions were examined on the same device and two hours were allowed for equilibration each after change of gas flow connections. When air and N₂ gases were connected, a linear gradient was observed. Zero oxygen solution dissolving 2mg/ml of RTDP was used as a reference, and the fluorescent signal was similar to the value from the chamber with the lowest O₂ concentration in the gradient.

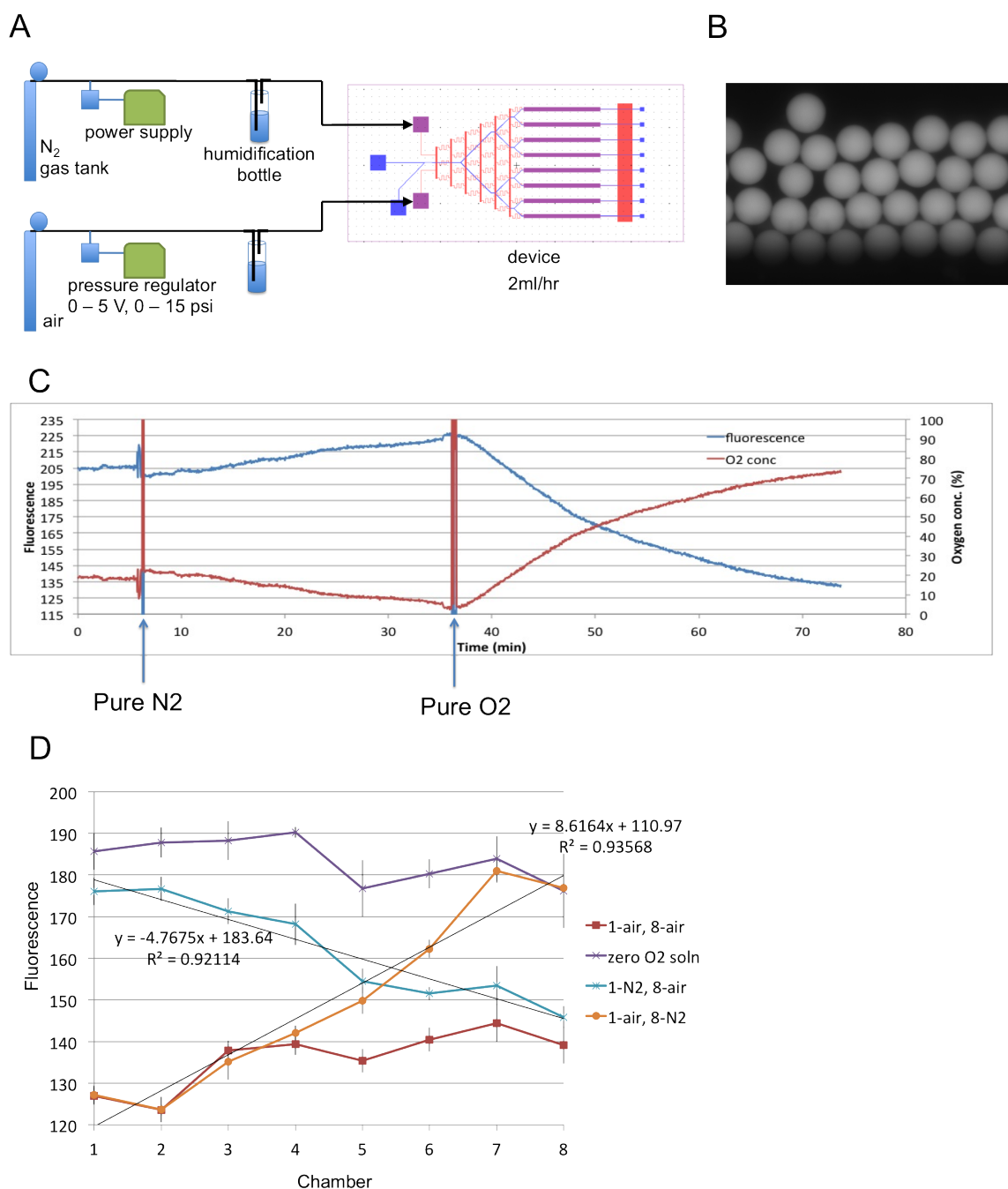


Figure 3.2: Oxygen gradient established in a multi-layered microfluidic device. (A) Connection of two gas flows to the microfluidic device through humidification bottles. (B) Gray scale image of droplets of RTDP solution in a chamber. (C) Change in fluorescence of RTDP droplets in real time. As gas flow changes, fluorescent signal changes as well. (D) Linear oxygen gradient microfluidically constructed across eight chambers.

3.3.3 Cultivation of murine fecal microbiota

The gastrointestinal tract of a mammalian host supports the growth of various microbial species with different oxygen tolerance and preference⁵⁰. Thus, providing limited amount of oxygen in well-localized environment can expand the repertoire of cultivable species of GI tract microbiota. A fecal sample was collected from a wild-type female mouse C57dl/6 and homogenized in tryptic soy broth to isolate the microbes. The microbial sample was diluted to generate initial cell density of 30 to 60 cells per droplet and cultivated under the oxygen gradient at 37°C for 24 hours. After the cultivation, droplet were retrieved from the device and analyzed by terminal restriction fragment length polymorphism (TRFLP) of 16S rDNA using MspI as a restriction enzyme. Each peak in TRFLP results usually represents a specific species of the community. Droplets from two adjacent chambers were combined for off-chip analysis (Figure 3.3A).

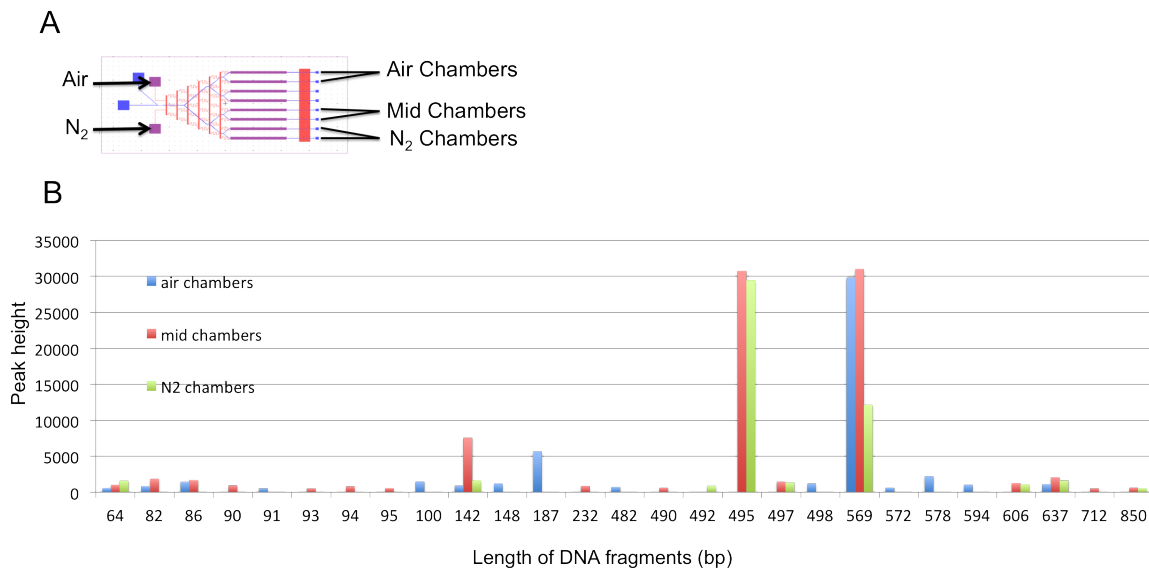


Figure 3.3: Cultivation of murine fecal microbiota under oxygen gradient. (A) Connection of gas flow to the device and droplet retrieval after cultivation. Data for the 3rd/4th chambers missing due to unsuccessful retrieval of droplets. (B) Results of TRFLP.

Our TRFLP results show that different enrichment occurred under different oxygen conditions (Figure 3.3B). For example, the fragment at 142bp represents a bacterial species that can grow well only in a microaerobic environment, whereas the fragment at 187bp represents a species enriched in the fully aerobic environment. The peak at 569bp implies a species whose growth is suppressed under the anaerobic condition. Similarly, the peak at 495bp suggests a species that cannot tolerate the aerobic condition. These results demonstrate that diversification of the oxygen concentration in the culture environment can expand the repertoire of cultivable microbial species from a microbial community.

For further demonstration of capability supporting the growth of species with various oxygen tolerance and preferences, several representative species from each group of strict anaerobes, facultative anaerobes, obligate microaerobes and obligate aerobes will be cultivated using the device. Oxygen concentration can be estimated according to the chambers where each microbial species proliferates.

For further demonstration of capability of the device supporting the growth of species with various oxygen tolerance and preferences, several representative species from each group of strict anaerobes, facultative anaerobes, obligate microaerobes and obligate aerobes will be cultivated. Oxygen concentration can be estimated according to the chambers where each microbial species proliferates.

3.4 Materials and Methods

3.4.1 Fabrication of microfluidic devices

Two glass channels were fabricated by photolithography processes as previously described⁸⁹. The pattern of a Cr mask was transferred to an AZ1518-coated glass wafer. The wafer was wet-etched by hydrofluoric acid, until the depth of the channel reach 50 μ m. Etched wafer was diced and electrochemically drilled in sodium hydrox-

ide solution for making inlets and outlets. $50\mu\text{m}$ -thick PDMS membrane was made by spin coating of 10:1 mixture of PDMS base and curing agent on a silicon wafer with 300 rpm for 90 seconds. One side of PDMS membrane and surface of glass channel for gas flow were treated by oxygen plasma using reactive ion etcher for bonding. After bonding of PDMS membrane and gas phase channel, the other side of PDMS and the surface of liquid phase channel were coated by Parylene. Parylene made the surface hydrophobic to make monodispersed droplets. In case of fabrication of the device designed for droplet retrieval from individual chambers, a PDMS block was attached to on top of outlets before Parylene coating. The PDMS block tightly holds Teflon tubes (i.d. $150\mu\text{m}$ and o.d. $360\mu\text{m}$) connected to outlets of individual chambers (Figure 3.4). Parylene-coated surfaces were bonded using UV glue. For the device designed for droplet retrieval, Teflon tubes were put through the PDMS block before UV gluing. After bonding, reservoirs were attached on top of the glass channel for liquid flow. The device was sterilized under UV at least one hour before use.

3.4.2 Droplet generation and retrieval

A perfluoropolyether polyethyleneglycol block copolymer surfactant (RainDance Technologies) was dissolved in fluorinated oil HFE-7500 (3M) at the final concentration of 2% wt/wt. Dissolved oxygen was purged from all liquid phase before

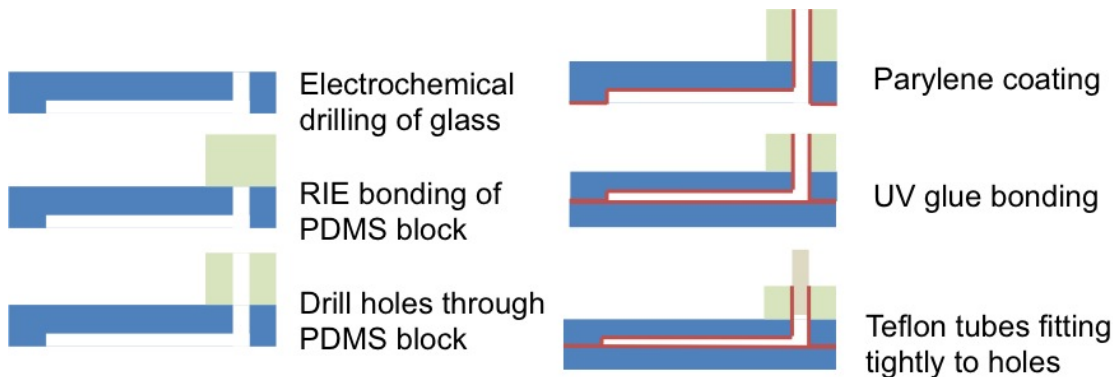


Figure 3.4: Construction of liquid channel outlets for droplet retrieval.

droplet generation by humidified nitrogen gas. In the experiments of oxygen concentration measurement, devices with one outlet in liquid flow channel were used, because droplets don't need to be retrieved. After the device was connected to the vacuum source, 50 μ l of oil and aqueous phase were added into inlet reservoirs. Using LabView interface, continuous vacuum was turned on, and the power of the vacuum was fixed at 200mmHg. After enough droplets were generated, vacuum was turned off and all reservoirs and connections were removed from the device as quickly as possible. Inlets and outlet of liquid phase channel were sealed with epoxy to prevent evaporation of oil and droplets during incubation.

In cultivation of murine fecal microbiota, the device designed for droplet retrieval was used for further analyses. Pressure was applied by syringe pumps to generate droplets, because the device has an outlet for each chamber which is connected to a Teflon tubing. The flow rates for oil and aqueous phase were set to 15 ml/hr and 10 ml/hr, as respectively. After enough droplets were generated, syringe pumps were turned off and all syringes were quickly detached from the device. Inlets and Teflon tubing were sealed with epoxy.

3.4.3 Oxygen gradient generation

A 99.8% dry N₂ cylinder, a 99% dry O₂ cylinder and house air were used. All gas lines were controlled by individual pressure regulators connected to power supplies. Gas flows were turned on at least 20 minutes in prior to connection of devices to fill humidification bottles and tubing. After connecting a device, pressure was maintained at 5 psig approximately. For generation of oxygen gradient, N₂ and house air were connected.

3.4.4 Measurement of oxygen concentration using RTDP solution

Ruthenium tris(2,2'-dipyridyl) dichloride hydrate was dissolved in zero oxygen solution (Cole Parmer) and deionized water at the final concentration of 2 mg/ml. After droplet generation, the device was connected to gas flows and placed under a fluorescent microscope. After allowing enough time (approximately two hours) to reach equilibrium, microscopic pictures were taken in gray scale at three different regions of each chamber and five droplets were cropped from each picture for image analysis. Therefore, brightness of fifteen droplets from each chamber was acquired, and the average and standard deviation was calculated by MATLAB.

3.4.5 Isolation and co-cultivation of murine fecal microbiota

Murine fecal sample was collected from a female wild type mouse C57dl/6. Within one day from collection of the sample, microbial community was isolated by adding 1ml of tryptic soy broth and homogenizing with a micropipette tip. Fecal debris in homogenized sample was removed by centrifugation with 2500 rpm for 5 minutes. The supernatant was transferred to a cryovial and 1ml of 50% glycerol was added. Cell density of the stock was estimated using a cell counting chamber. Before the encapsulation, the cell stock was diluted as desired. Remaining stock was stored at -80°C for further analysis.

3.4.6 Terminal restriction fragment length polymorphism

Genomic DNA was extracted from the culture or cell stock using MagNA Pure Compact (Roche). The sample was mixed with 150µl of bacterial lysis buffer (Roche), lysed by bead beating, treated with Proteinase K and processed by MagNA Pure Compact machine for isolation of genomic DNA. The elution volume was 50 µl. Concentration of DNA was measured using NanoDrop.

Metagenomic DNA extracted as described above was also used as a template of

PCR reaction for TRFLP. Three replicates of 25- μ l reaction mixture were prepared with 70ng of genomic DNA, 6-FAM labeled universal 8F primer (5'-AGA GTT TGA TCC TGG CTC AG-3') and non-labeled universal 1492R primer (5'-GGT TAC CTT GTT ACG ACT T-3'). Amplicon was combined, purified (PCR purification kit, Qiagen) and measured by NanoDrop. 300ng of purified amplicon was digested with MspI for 2 hours and purified with nucleotide purification kit (Qiagen) for not losing small fragments of DNA. Digested samples were submitted to University of Michigan Sequencing Core for genotyping capillary electrophoresis. Raw data of electrophoresis was analyzed by peak labeling of Peak Scanner v.1.0 software (ABI Biosystems). Labeled peaks were plotted by an in-house program coded in Python and MATLAB.

CHAPTER IV

Development of Microfluidic Devices for Automated Sorting of Droplets

4.1 Summary

Microfluidically generated droplets can provide well-localized environment for cultivation of microbes in a highly parallel manner. Two possible applications include the co-cultivation of complex natural microbial communities and screening of strain libraries for microbial engineering. For each case, further parallelization and automation of the droplet-enabled technology is highly desirable. In this work, we develop a simple and robust device for incubation of millions of droplets for a week using a microcentrifuge tube and combine it with a microfluidic device for automated sorting. Droplets are stable enough to maintain their monodispersity during incubation and transport from or to a device. Automated sorting was performed hydrodynamically based on the fluorescent image analysis of droplet images representing cell density after cultivation. As an initial application, the technology will be utilized for high-throughput screening of engineered *E. coli* libraries for improved isobutanol-tolerance for more efficient biofuel production.

4.2 Introduction

Recent advancements in sequencing based microbial ecology have resulted in an explosive increase in the number of microbial species identified from natural communities⁸³ and revealed the complexity of natural microbiota. The huge gap between the number of microbial species present in nature and that of cultivated species requires revolutionary improvement in the throughput of laboratory cultivation. While the total number of microbial species is now estimated to be 10^6 , only a few thousands of them have been isolated in lab culture. High-throughput approaches for microbial cultivation and screening may facilitate the isolation of microbial species that play ecologically important roles in a complex natural microbial community.

On the other hand, artificial microbial libraries, in addition to complex natural microbiota, also require high-throughput screening method. Libraries generated by various protein and genome engineering techniques for directed evolution contain 10^4 to 10^{12} variants³⁵. Screening for highly functional strains from such a large population can be an extremely laborious and tedious task, and consequently, be the rate-determining step in the whole process. For improvement of throughput, various screening technologies were developed, and the culture-complemented assay is one of the frequently used methods^{99,88}. Therefore, coupled with high-throughput cultivation in droplets, automated screening can be a powerful tool for engineering of enzymes and microbial strains.

We previously developed a microfluidic device for droplet-enabled co-cultivation to investigate symbiotic interactions in a microbial community⁸⁹. Microfluidically generated droplets provided well-localized and parallel environment for microbial cultivation. We could stably incubate about 1400 droplets in a glass device. To apply the technology to the investigation of complex natural microbiota or artificial libraries with a large population, it is highly desirable to develop the capability of handling a much larger number of droplets and incorporate automated high-throughput screen-

ing downstream of cultivation.

Various microfluidic approaches have been developed for high-throughput screening of droplets. Path of droplets can be controlled dielectrophoretically^{4,3,21,85} and hydrodynamically^{1,104,19}. Screening criteria used in these research were mostly fluorescent signal^{3,1} and size of droplets^{104?}. For screening of microbial strains based on growth, fluorescent signal detection can be easily combined with microbial cultivation by heterologous expression of a fluorescent protein in microbes. However, detecting fluorescent signal from individual cells in droplets for automated sorting requires higher magnification than detection of the signal from molecules dissolved in droplets.

In this work, we develop a simple and robust platform connecting microfluidic devices and a microcentrifuge tube that is able to incubate 10^6 droplets at once. After incubating millions of well-localized cultures, we transfer the droplets stably to a microfluidic device made of polydimethylsiloxane (PDMS) for automated sorting. The sorting device is composed of three parts including droplet detection, spacing and sorting. Droplets carrying well-grown microbial cultures are sorted by control of flow resistance, according to the results of image analysis at the detection part followed by spacing. This technology will be utilized to screen for highly isobutanol-tolerant *E. coli* strains from library consisting of up to 10^{11} variants generated from a multiplex automated genome engineering.

4.3 Results and Discussion

4.3.1 Handling a large number of droplets

For parallelizing further droplet-enabled cultivation, stable incubation of a larger number of droplets is necessary. In our previous research, the frequency of droplet generation was as high as 500 Hz, but the small chamber of the device could hold

only 1400 droplets at once. In order to overcome this limitation, here we develop a simple platform that allows incubation of up to 106 droplets using an Eppendorf tube (Figure 4.1A) and a robust way to transfer a large number of droplets from a device to the tube or vice versa (Figure 4.1B). Droplets are stabilized by a biocompatible surfactant, perfluoropolyether polyethyleneglycol⁵², and can be incubated in a tube for several days without merging. A Teflon tube with hydrophobic surface and the inner diameter equivalent to microfluidic channel is used to connect the incubation tube and a device dimension. It is plugged tightly into an outlet or an inlet of a PDMS device and shear force is minimized to avoid breakup of droplets during the transfer process (Figure 4.1C).

The PDMS device for droplet generation comprises a slanted T-junction for droplet generation and a small chamber for confirmation of monodispersity of droplets. The slanted T-junction is able to generate droplets with a single vacuum line connected to the Eppendorf tube and the device outlet, instead of multiple lines of pressure at the inlets. Increasing power of the vacuum led to increase of the frequency of droplet generation and subsequently the number of droplets in the chamber. The achievable range of frequency is 1-1000 droplets/sec and volume of droplets was 1nl. During continuous generation of droplets, monodispersity of droplets are monitored in a chamber where the flow rate is decreased due to the increased channel width. Droplets are then stably transferred to the Eppendorf tube.

After the droplets filled the tube, the vacuum is removed and the droplet generation stops immediately. The density of HFE-7500 is 1.61g/ml and its volumetric flow rate is about twice as high as that of the aqueous phase. As a result, the tube contains HFE-7500 at the bottom which is twice the volume of droplets at the top. To provide enough amount of air during incubation, the bottom layer can be pushed out through the Teflon tube, with about 30 μ l of oil phase remaining to retain stability of the droplets. Droplets decorated with the surfactant do not coalesce due to

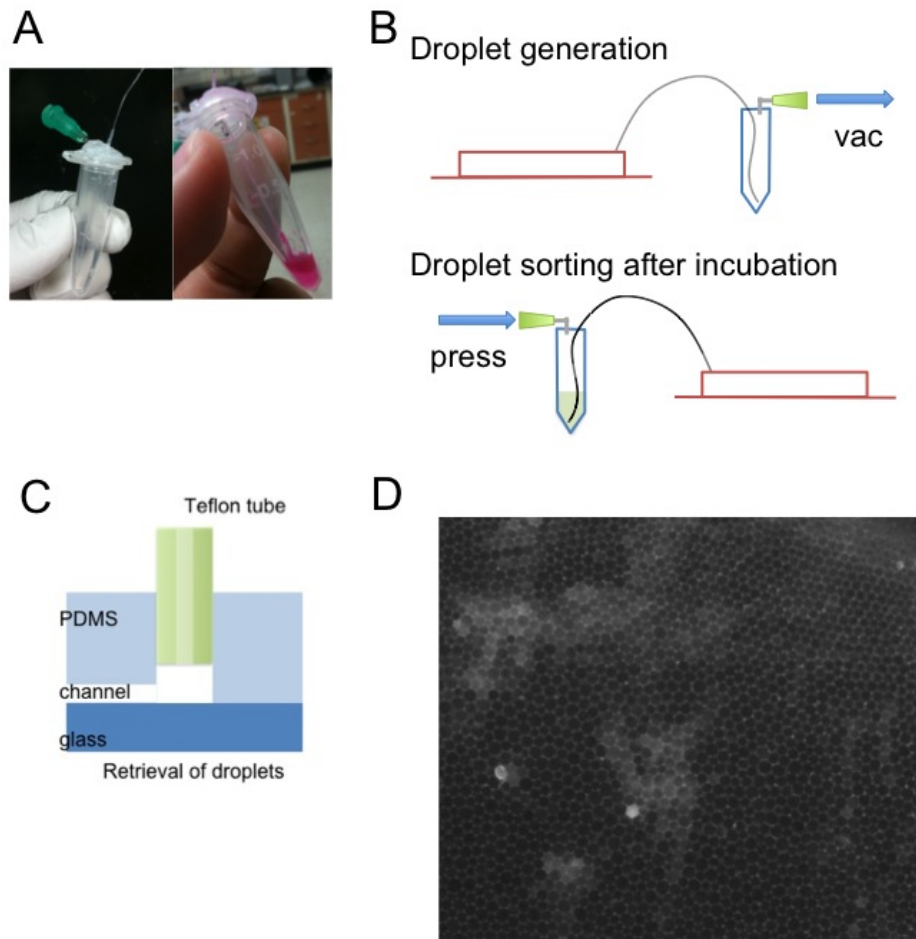


Figure 4.1: Device-centrifuge tube connection for increasing incubation throughput. (A) Pictures of an Eppendorf tube used for droplet incubation. Left - A tube without droplets. Right - A tube containing droplets of rhodamine A solution. (B) Schematics of droplet generation and reinjection for automated sorting after incubation. (C) Connection of Teflon tube to a PDMS device for droplet retrieval. (D) Picture of monodispersed droplets after reinjection.

Marangoni effect¹¹, which keeps oil phase between droplets from drainage. In addition to preventing droplet coalescence, the oil phase between droplets inhibits evaporation of droplets. Microdroplets with volume of 1nl evaporate quickly within one minute when they are not surrounded by oil. Therefore, the remaining small amount of oil in the tube serves as a reservoir during long incubation exceeding one day. Without any leftover of oil, the droplets shrink and are not monodispersed after incubation of 36 hours.

After incubation in the Eppendorf tube, droplets are stably reinjected to a microfluidic device (Figure 4.1B). Applying pressure of about 1psig to the tube pushes droplets into a PDMS device through the Teflon tube. Droplets remain monodispersed after the reinjection process (Figure 4.1D).

4.3.2 Hydrodynamic droplet sorting based on bacterial growth

To facilitate analysis downstream of parallel droplet-enabled cultivation for various applications, we have developed a microfluidic device for automated hydrodynamic droplet. The device consisted of T-junction for droplet spacing and a Y-shaped branch for droplet sorting (Figure 4.2A). Appropriate spacing at the junction allows enough time to process droplet images for estimation of cell growth before path selection at the Y-shaped branch for droplet screening. Spacing between droplets is precisely controlled by changing the flow rates of droplets and spacing oil. Although a high flow rate of spacing oil enables large spacing, not every combination of the two flow rates is allowed. Specifically, the flow rate of spacing oil can be higher than that of incoming droplets because the flow resistance downstream of the spacing junction is lower than that of upstream. However, there exist a minimum flow rate of droplets to keep the spacing oil from pushing droplets back. As the flow rate of spacing oil increases, the required minimum rate of droplets increases, but the ratio between two flow rates is not a constant. For example, large spacing is achieved with 10ml/hr of

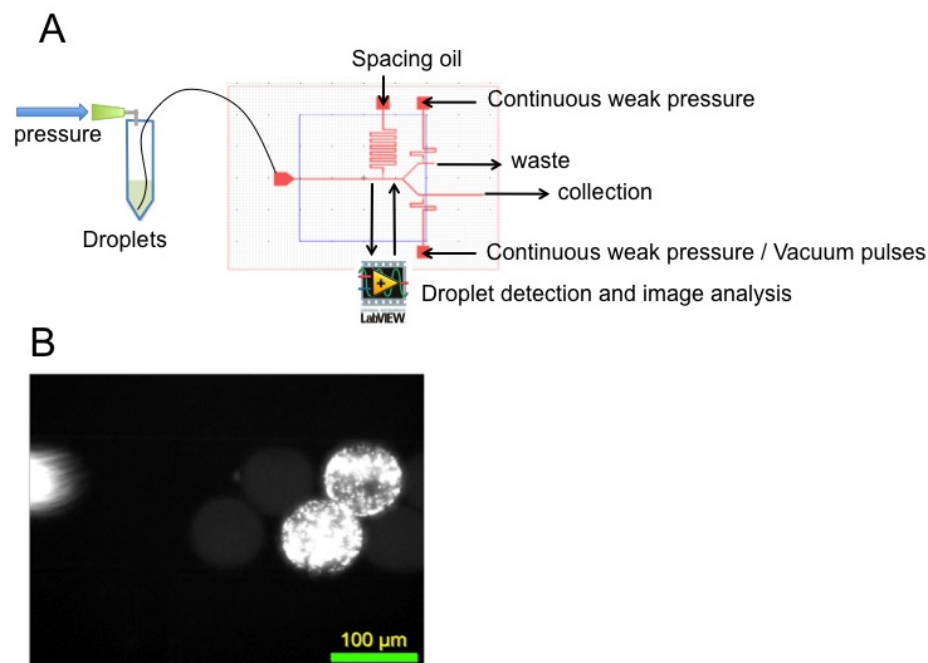


Figure 4.2: Automated droplet sorting. (A) Device design and operation for automated sorting of droplets. (B) Spacing of droplets at the T-junction. *E. coli* K12 expressing GFP was encapsulated and cultivated. Droplets provided well-localized environment for microbial cultivation.

oil and 5ml/hr of droplets as minimum, whereas 5ml/hr of oil and 4ml/hr of droplets enable small spacing (Figure 4.2B).

Proper balance between pressures on the spacing oil and droplets allow a droplet to stay right before the junction for a few seconds. A fluorescent image of cells in the droplet is captured at this region and a LabView program determines whether the fluorescent value exceeds a threshold or not while the droplet flows to the Y-shaped branch. Without any intervention, the droplet goes to the waste line at the branch because the waste line has lower flow resistance. When a droplet carries well-grown cells and consequently has high fluorescence, a vacuum pulse is applied to the collection line and the droplet is retrieved.

To test and optimize the system, sorting of droplets carrying well-grown cells from empty droplets was performed. YFP-labeled *E. coli* cells were cultivated in a highly parallel manner using an Eppendorf tube. Based on the Poisson distribution, about

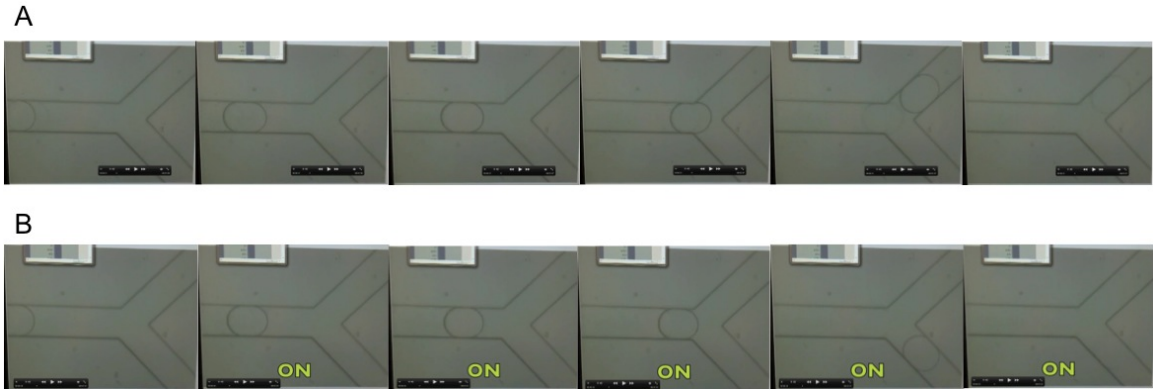


Figure 4.3: Picture sequences captured from a video clip showing droplet sorting. (A) An empty droplet goes to the waste line with no intervention. (B) A droplet exceeding threshold value of fluorescence is collected by a vacuum pulse applied to the collection line. The picture sequence used in this figure was captured during the sorting with empty droplets for video recording.

70% of the droplets were empty when the average number of cells per droplet was 0.3. After 24-hr cultivation, droplets were reinjected and those with high cell density were sorted into the collection line based on fluorescent signal detected by LabView. When an empty droplet passed the detection region, no intervention was performed and the droplet went to the waste line (Figure 4.3 A). If a droplet had high fluorescent signal due to encapsulated cells, the LabView program signaled its passing. According to the signal, a vacuum pulse was applied to the collection line and the corresponding droplets was retained (Figure 4.3B).

4.4 Materials and Methods

4.4.1 Connecting microcentrifuge tubes for incubation of a large number of droplets

For storage and incubation of large number of droplets, an Eppendorf tube was used. Two holes were drilled on the lid of a sterile Eppendorf tube by a press drill. A Teflon tube (i.d. $150\mu\text{m}$ and o.d. $360\mu\text{m}$, IDEX Health and Science) and a steel

syringe tip were fixed at the holes using UV glue. One end of the 5cm-long Teflon tube touched the bottom of the Eppendorf tube.

4.4.2 Fabrication of microfluidic devices

For droplet generation and automated sorting, polydimethylsiloxane (PDMS) devices were fabricated using SU-8 molds. SU-8 molds were made using general photolithography processes. A 4" silicon wafer was etched by buffered hydrofluoric acid for 10 minutes. SU-8 2015 (Microchem) was spun at 2000 rpm on the wafer at the final thickness of $50\mu\text{m}$ and baked at 65°C for 3 minutes and at 95°C for 9 minutes. A device design was transferred to SU-8 layer using a mask aligner with UV exposure of 16.5 second. After post-exposure bake at 95°C for 10 minutes, the pattern was developed by immersion in SU-8 developer (propylene glycol monomethyl ether acetate) for 10 minutes with slight agitation. The wafer was rinsed with isopropanol and dried.

PDMS base and curing agent (Dow Corning) were mixed at 10:1 ratio and poured on top of SU-8 mold described above. After degassed in a vacuum desiccator for an hour, it was cured at 70°C for an hour. The cured PDMS was carefully peeled off from the mold and cut into individual devices. Holes for inlets and outlets were drilled by precision needle tips. The PDMS channel was rinsed with isopropanol and treated with oxygen plasma for a minute in a reactive ion etcher. A glass slide was treated at the same time. Forward and reflective powers were 26 and 4, respectively. Immediately after the plasma activation, the PDMS channel was covered with the glass slide and the device was heated at 75°C for 2 hours.

4.4.3 Droplet generation

Teflon tube of the Eppendorf tube was plugged into the outlet hole of droplet-generating device. Two syringes open to the atmosphere were connected to inlets and

used as reservoirs for aqueous and oil phases. A perfluoropolyether polyethyleneglycol block copolymer surfactant⁵² (RainDance Technologies) was dissolved in fluorinated oil HFE-7500 (3M) at the final concentration of 2% wt/wt. House vacuum was connected to the needle tip of the Eppendorf tube for droplet generation and the intensity of vacuum was controlled by a vacuum regulator.

After generation of enough number of droplets, the vacuum was turned off first and detached from the Eppendorf tube. Next, the Teflon tube is pulled out from the outlet. Excessive oil phase in the Eppendorf tube was carefully pushed out using a syringe, but small amount (about 30 μl) of oil was left for maintaining stability of droplets. The needle tip of the tube was sealed with Parafilm and the tube was incubated at any temperature as needed.

4.4.4 Droplet reinjection, spacing and sorting

All processes of droplet reinjection, spacing and automated sorting was controlled by a LabView program consisting of two modules for flow control and image analysis, and performed on the stage of an inverted fluorescent microscope (Nikon). Syringes were connected to three inlets for waste line, collection line and spacing line and filled with HFE-7500 without surfactant. After filling the channel with HFE-7500, the Eppendorf tube was connected to the device by plugging Teflon tube into the inlet for droplet reinjection. An empty syringe was connected to the needle tip of the Eppendorf tube. Without any operation of LabView controller, HFE-7500 was slightly pushed into the device from the three inlets of oil phase by gravitational force. House air and vacuum was used for pushing and pulling of droplets and oil. The flow control part of the LabView program digitally controlled the voltage supplying power to pressure and vacuum regulators connected to individual lines for droplet reinjection, spacing and collection.

The image analysis part of the LabView program has two steps of processing.

First it detects the boundary of droplets and then calculates the fluorescent signal from the droplet only when droplet boundary is detected. This image analysis takes place right before a droplet passes the spacing branch, so that the spacing region of the device was monitored with 20x magnification. When the fluorescent signal from a droplet exceed a preset threshold value, the LabView program sends signal to flow control part to give a vacuum pulse to the syringe connected to the collection line.

4.4.5 Automated sorting of droplets with fluorescently labeled *E. coli*

YFP-cat gene cassette was integrated to intC locus of the chromosome of *E. coli* EcHW24 strain by P1 transduction. LB media supplemented with chloramphenicol and 2mM IPTG for YFP expression was inoculated with EcHW24 intC::YFP-cat and incubated at 30°C. The overnight culture was diluted with the same LB media used for seed cultivation. The dilution ratio was determined by estimation of cell density using UV spectrometer. To prepare cells for droplet sorting from empty droplets, the seed culture was diluted 5000 times. The diluted cell culture was encapsulated, incubated and sorted as described.

CHAPTER V

Droplet-Enabled Co-Cultivation of Tunicate Microbial Communities

5.1 Summary

Certain marine invertebrates have been known to harbor microbial communities that produce drug and antibiotic molecules⁹¹. For instance, ET-743, an anticancer drug, is a natural product originally purified from the tunicate *Ecteinascidia turbinata* and is believed to be a secondary metabolite secreted by a symbiotic bacterium, *Candidatus Endoecteinascidia frumentensis*^{81,90,93}. The gene cluster for the biosynthesis of ET-743 in the microbe of interest was identified previously, but the bacterium has never been cultivated in laboratory so far. Due to the extremely low yield of extraction from the natural source and an inability to culture *C. frumentensis*, mass production of ET-743 currently depends on a costly semi-synthetic pathway²⁶. In this work, we isolate the microbiota from tunicates and co-cultivate them in micro-droplets in an attempt to obtain the drug-producing species and to elucidate the microbial interactions in the tunicate microbial community. The droplet co-cultivation platform we previously developed is utilized for the investigation of the tunicate microbiota. Isolated tunicate microbiota are co-cultivated in conventional lab rich media and seawater collected from the original habitat of tunicates. Grown co-cultures are re-

trieved from the device and characterized by Terminal Restriction Fragment Length Polymorphism (TRFLP) and sequencing of 16S rRNA genes. Co-cultures developed under conditions closer to its native environment show higher diversity compared to those derived from the lab medium. Our ongoing efforts include further optimization of the co-cultivation environment by exploring microaerobic conditions and different media, and improving the initial microbiota isolation process.

5.2 Introduction

Marine invertebrates have been investigated as sources of drug molecules and microbes living in those animals are believed to be drug producers in many cases⁹¹. Ecteinascidin 743 (ET-743), an antitumor agent, was first isolated from *Ecteinascidia turbinata* in the late 1960s^{94,95} (Figure 5.1A). The yield of extraction from natural source is extremely low, so that its mass production currently depends on costly semisynthetic pathway starting from safracin B molecule produced by *Pseudomonas fluorescens*²⁶ (Figure 5.1B). As metabolites similar to ET-743 have been known to be produced by bacteria, ET-743 also has been considered to be of microbial origin^{90,91}. There have been significant efforts for phylogenetic analysis of 16S rRNA from microbial communities dwelling in tunicate, and a γ -proteobacteria *Candidatus Endoecteinascidia frumentensis* was the only species found from every *E. turbinata*, regardless of sites where they were collected⁹⁰. Abundance and presence at all sites of *C. frumentensis* imply that the species is a potent producer of ET-743.

Although *C. frumentensis* is believed to synthesize ET-743 and to be most abundant in *E. turbinata*, it has never been cultivated in vitro and isolated as a pure culture. Accordingly, current studies are limited to in vivo analysis or metagenomic/metaproteomic approaches not requiring isolation of the species. Microbial diversity in tunicates collected from different sites was systematically investigated using denaturing gel gradient electrophoresis and phylogenetic analysis of 16S rRNA

sequences⁹⁰. In addition, Moss and his coworkers performed fluorescent in situ hybridization using several different probes hybridizing with 16S rDNA of *C. frumentensis* and confirmed that it is highly possible to be an endosymbiont using scanning electron microscope images⁸¹. More direct evidence showing that *C. frumentensis* is a drug-producer was found by metagenomic and metaproteomic approach identifying biosynthesis pathway of ET-743 in *C. frumentensis*⁹³.

Previously we developed a microfluidic device for droplet-enabled co-cultivation of microbial communities to investigate microbial symbiotic interactions⁸⁹. We fabricated a microfluidic device that could readily encapsulate and co-cultivate subsets of a community, using aqueous droplets dispersed in a continuous oil phase. To demonstrate the effectiveness of this approach in discovering synergistic interactions among microbes, we tested it with a synthetic model system consisting of cross-feeding *E. coli* mutants, which were labelled with fluorescent proteins.

In this work, we perform droplet-enabled co-cultivation of natural microbial communities isolated from *E. turbinata*, which have not been intensively investigated by cultivation approach. For co-cultivation and characterization of natural microbiota, further genetic analysis is required because microbes are not labeled and identified. The droplets were collectively retrieved from devices after cultivation and analyzed by terminal restriction fragment length polymorphism (TRFLP) and 16S rRNA sequencing. TRFLP results showed that droplet-enabled co-cultivation using various

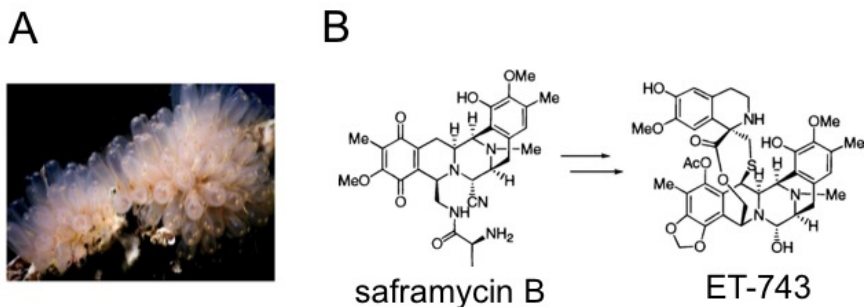


Figure 5.1: Picture of tunicate (A) and molecular structure of ET-743 (B).

culture media enriched different microbial species and they could be identified by comparison with 16S rRNA sequencing results.

5.3 Results and Discussion

5.3.1 Sequencing of 16S rDNA library from tunicate sample

To confirm the presence of *C. frumentensis* in a tunicate sample, metagenomic DNA was extracted from homogenized frozen tunicate sample. 16S rDNA library was sequenced and analyzed phylogenetically using Ribosomal Database Project, Blast and ClustalW (Figure 5.2). 19 operational taxonomic units (OTU) were identified at 97% of similarity. The most abundant OTU had more than 99% of sequence similarity to *C. frumentensis* (GenBank ID: DQ831976.1), agreeing with the results of other studies. Other OTUs include α -proteobacteria Rhodobacteraceae, γ -proteobacteria Ectothiorhodospiraceae, a few unclassified γ -proteobacteria and a few unclassified bacteroidetes. The sequences were utilized for identification of peaks in TRFLP results.

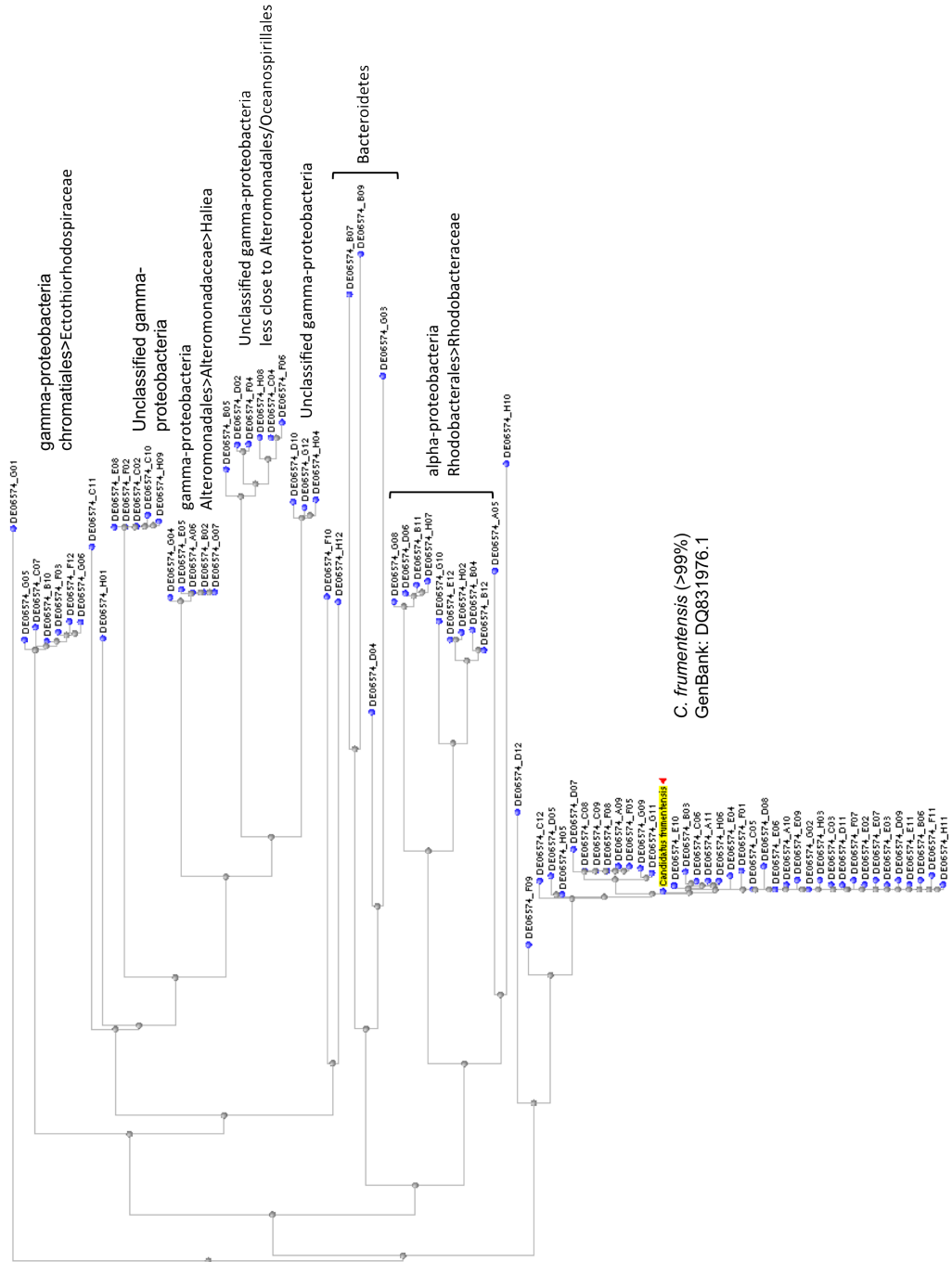


Figure 5.2: Phylogenetic tree of 16S rRNA sequences. Sequence of *C. frumentensis* added as a reference is highlighted in yellow.

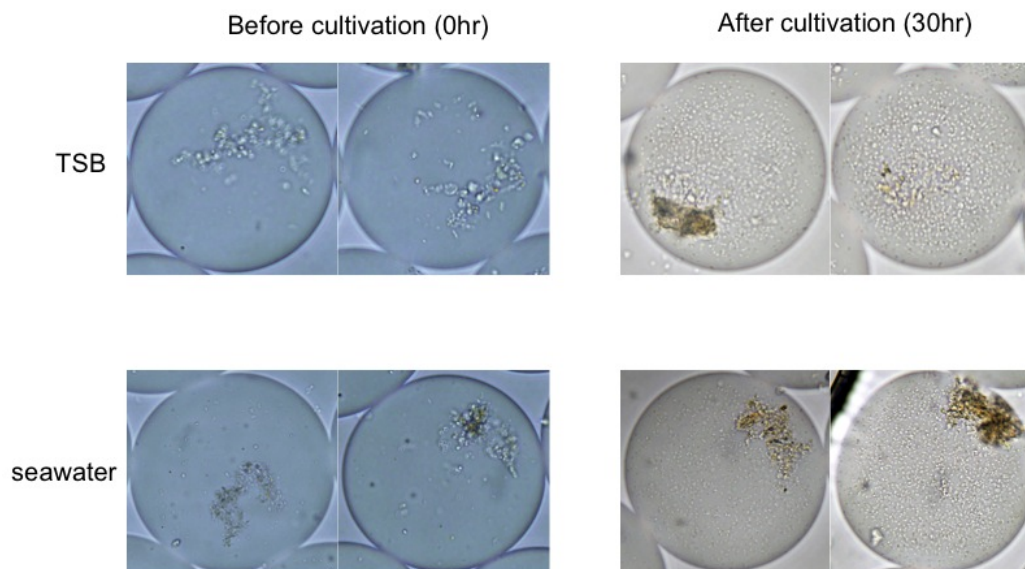


Figure 5.3: Droplet-enabled co-cultivation of a tunicate microbial community in TSB and seawater. Left - Microscopic pictures of droplets encapsulating a tunicate microbial community before the cultivation. Right - Microscopic pictures of droplets after 30-hour cultivation. Reddish clusters are unfiltrated debris of tunicate tissue.

5.3.2 Droplet-enabled co-cultivation of tunicate microbiota

To isolate a microbial community for droplet-enabled co-cultivation, fresh *E. turbinata* tissue was blended within two days after tunicate collection. Blended tissue was filtrated through $5\mu\text{m}$ -pore membrane to remove large debris. After estimation of cell density using a cell counting chamber, the microbial community was diluted to have the initial cell density of 50 - 100 cells/droplet using two different media, TSB and seawater. TSB and seawater provide nutrient-rich and close-to-nature environments, respectively. The fraction of droplets containing well-grown microbes were reduced from about 60% to about 5% by decreasing initial cell density to 10 cells per droplets. The growth of microbes was monitored by microscopy (Figure 5.3). While microbes were grown fast in TSB media, culture in seawater showed morphologically more diverse microbes. During the cultivation, tunicate tissue debris was clustered in most of droplets.

After 30-hour cultivation, about 800 droplets were collectively retrieved from each device and analyzed by TRFLP using MspI as a restriction enzyme (Figure 5.4). The 16S rRNA sequences from the library of the community stock were digested in silico and compared with TRFLP results for identification of peaks. Comparing two genetic analyses, most major peaks of TRFLP were clearly identified. In both cultures, *Pseudomonas* and *Vibrio* were amplified most. In seawater cultivation, α -proteobacteria was enriched additionally.

In order to see the effect of different cultivation methods and media, culture environment was more diversified. In addition to pure TSB media and seawater, a mixture of seawater and TSB media at the final concentration of 30% v/v was prepared because a medium with low nutrient may help some microbes present in natural communities to grow. Furthermore, cultivation in a conical tube and droplet cultivation followed by conical tube cultivation were compared with droplet-enabled co-cultivation. In the combined culture, the population of the microbial community was first perturbed in droplet cultivation and then amplified in a conical tube. Eight different combinations of media and culture methods were tried and analyzed (Figure 5.5). TRFLP results demonstrates that cultivation in different media and different culture methods enriches different microbial members from a microbial community. No common trends were observed in the eight cultivations.

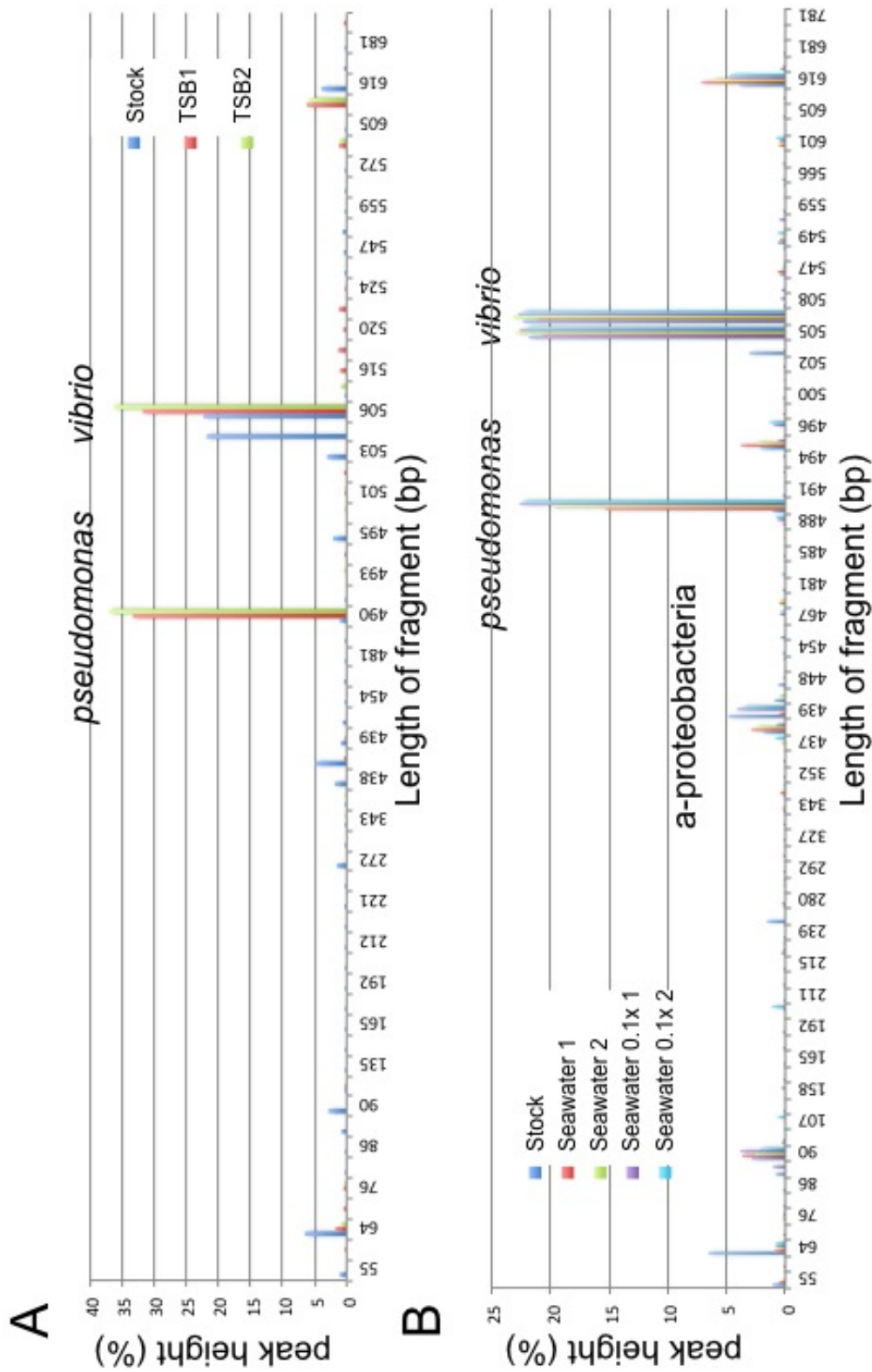


Figure 5.4: TRFLP results of droplet-derived co-cultures. (A) TRFLP of co-cultures in TSB media. Results from microbial community stock and two replicates of device cultivation are plotted. (B) TRFLP of co-cultures in seawater. Results from the microbial community stock, two replicates of seawater culture and two replicates of seawater culture with lower initial cell density are plotted.

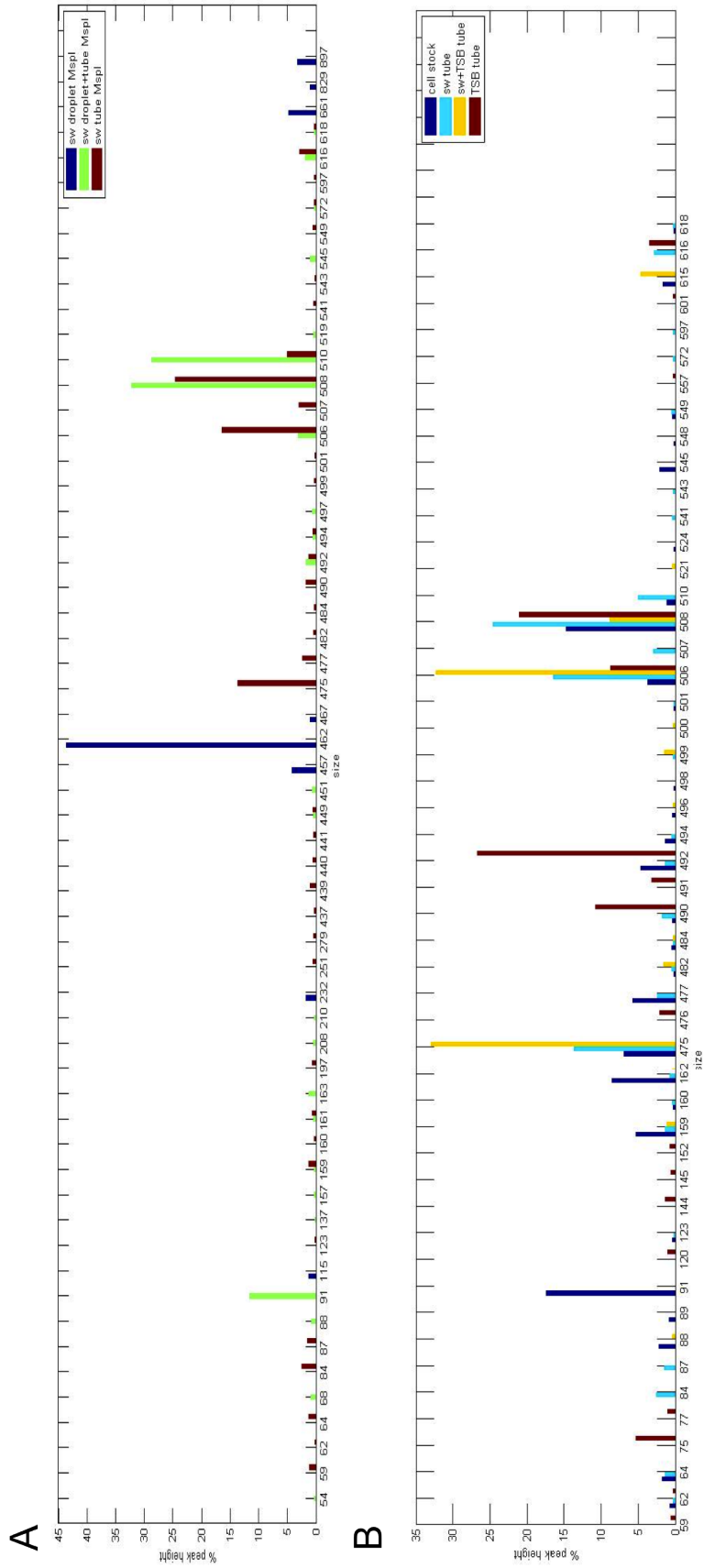


Figure 5.5: Comparison between culture methods and culture media. (A) TRFLP peaks of droplet cultivation, combined cultivation and conical tube cultivation in seawater. (B) TRFLP peaks of the community stock and conical tube cultivation in seawater, combined media and TSB media.

5.3.3 Isolation of microbes from tunicates

Based on the sequence of the OTU clustered with *C. frumentensis*, *C. frumentensis* should be represented as a 503-bp and 824-bp peak in TRFLP with MspI and RsaI digestion, respectively. In the previous co-cultivation experiments, enrichment of *C. frumentensis* was not observed. One possible reason for the absence of the species was that it is due to the variation of tunicate samples collected at different seasons. In order to examine this possibility, four different tunicate samples collected from November 2010 to August 2011 were analyzed (Figure 5.6). Although the relative abundance of populations was slightly different from a sample to another, most of species are present commonly in four tunicate samples and *C. frumentensis* was not observed.

Given that the 16S rRNA sequence of *C. frumentensis* was very abundant in metagenomic DNA prepared from tunicate without isolation of a microbial community, we speculated that *C. frumentensis* was not isolated effectively by mechanical blending. Two tunicate samples collected at the same time were processed using blending followed by filtration for isolation of a microbial community and homogenization without isolation of microbes. 16S rDNA amplified from two samples was analyzed by TRFLP. Only in the sample without isolation, the peaks representing *C. frumentensis* were observed (Figure 5.7). The isolation using mechanical blending is not enough to retrieve *C. frumentensis* from tunicate tissue. This is also indirectly supported by the SEM image showing that many microbes living in tunicate are endosymbiont. Therefore, a better isolation process without reducing viability is required for enrichment of *C. frumentensis*.

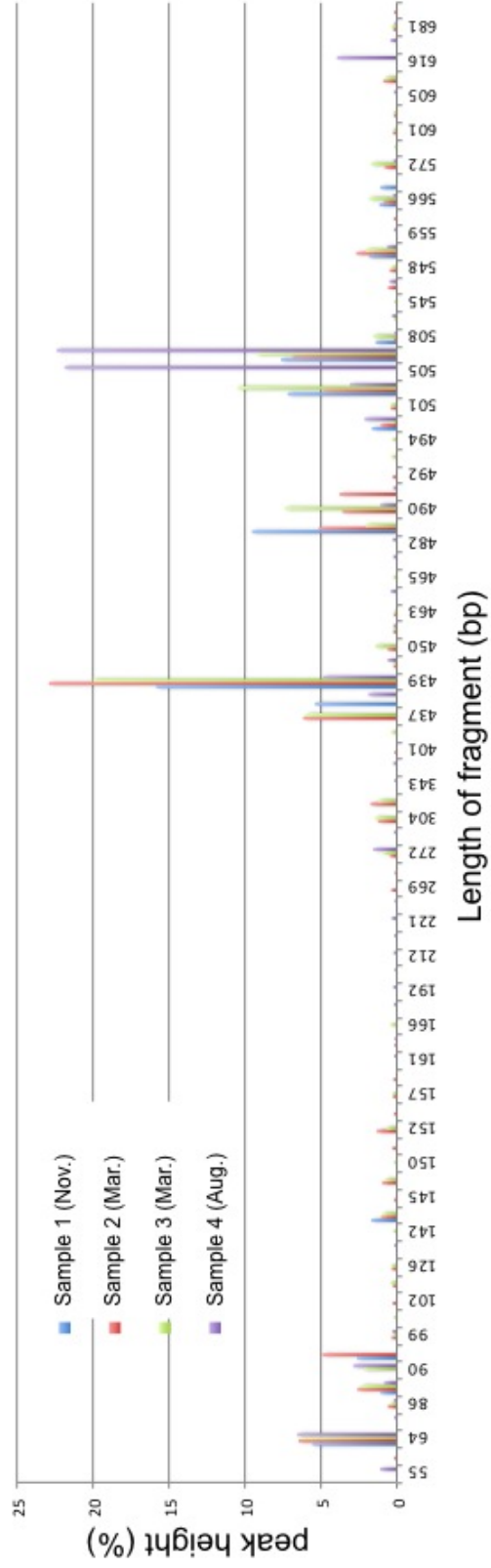


Figure 5.6: TRFLP results of tunicate samples collected from different seasons.

5.4 Materials and Methods

5.4.1 Microfabrication

We used glass devices. Channels were fabricated using general photolithography processes as described in the previous paper⁸⁹. A glass wafer was prepared with Cr-Au deposition and AZ1518 spin coating. The pattern of the Cr mask was transferred to the AZ1518-coated glass wafer with the UV exposure of LI 300 for 30 seconds. After developing for 1 minute in MF319 developer, Au and Cr were etched for 2 minutes. The glass wafer was wet-etched by HF, until the depth of the channel reach 50 μm . The channel depth was measured periodically by depth profiler during the etching process. After dicing the individual devices, holes for inlets and outlets were electrochemically drilled in sodium hydroxide solution. To make the surface hydrophobic, a 2 μm -thick Parylene film was deposited on the channel and a cover slip. Afterwards, the channel and the cover slip were bonded with UV glue. Glass tubes were attached with UV glue at the holes as reservoirs of inlets and outlets, and syringe tips were fixed to the oil inlet and outlet reservoirs with epoxy to connect the device to vacuum source and oil reservoirs. Before using the devices for the cultivation, all devices were exposed to UV for at least one hour for sterilization. All devices were regenerated after each use. They were heated in a 540 °C furnace for 2 hours, followed by cleaning in Piranha solution of $\text{H}_2\text{O}_2:\text{H}_2\text{SO}_4 = 1:2$. Parylene coating, bonding with UV glue, attaching reservoirs and sterilization were repeated as described above.

5.4.2 Isolation of microbial community from tunicates

Tunicates were collected at Florida Keys and shipped alive in seawater. Within one day from the shipment of the specimen, microbial community was isolated from the tunicate by grinding and encapsulated in droplets for cultivation. A kitchen

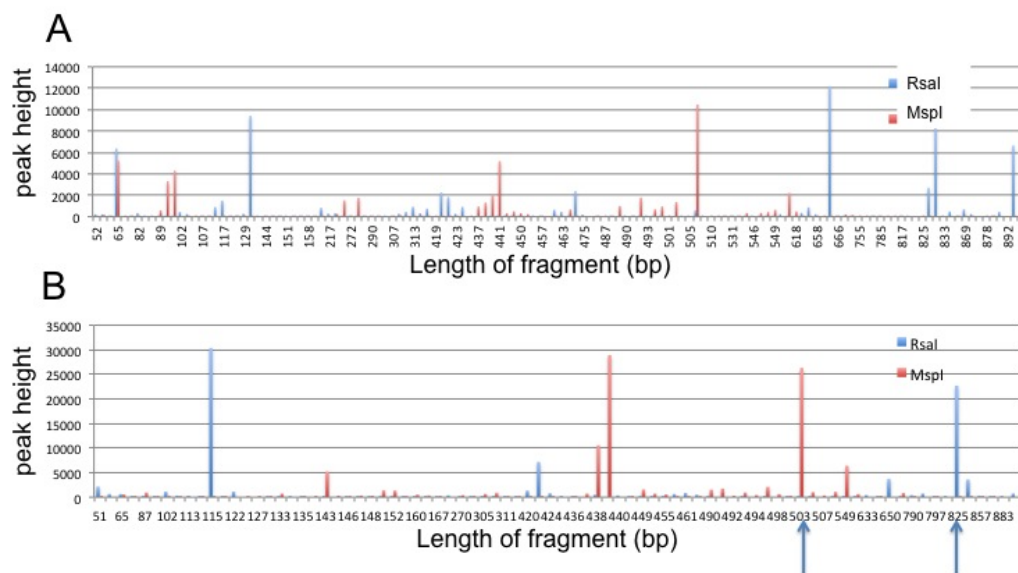


Figure 5.7: TRFLP results of tunicate microbiota prepared by different isolation methods. *C. frumentensis* has peaks at 824bp in RsaI (blue) digestion and at 503bp in MspI (red) digestion. (A) TRFLP of 16S rDNA amplified from microbiota after isolation by mechanical blending. (B) TRFLP of 16S rDNA amplified from microbiota not isolated from tunicate tissues. Peaks representing *C. frumentensis* are indicated by arrows.

blender used for grinding was rinsed with 70% ethanol thoroughly and sterilized by UV for 30 minutes. After grinding, the sample was filtrated through a membrane with 5 μm pores. Microbes in filtrated sample were harvested by centrifugation with 10000 rpm for 10 minutes. The supernatant was sterilized by filtration through 0.2 μm -pore membrane and the pellet was resuspended in 1ml of sterilized supernatant and 1ml of 50% glycerol. Cell density of the stock was estimated using a cell counting chamber. Before the encapsulation, the cell stock was diluted as desired. Remaining stock was stored at -80°C for further analysis.

5.4.3 Encapsulation, cultivation and monitoring of microbes

A PFPE-PEG block copolymer surfactant⁵² (RainDance Technologies) was dissolved in fluorinated oil HFE-7500 (3M) at a final concentration of 2% wt/wt. The oil phase was supplied in a syringe connected to the device. After the device was con-

nected to the vacuum source, 30 μl of diluted cell mixture was added into the aqueous-phase inlet reservoir. Using LabView interface, continuous vacuum was turned on, and the power of the vacuum was increased gradually to 150-300 mmHg. After enough droplets were generated, vacuum was turned off. All syringes, connections and reservoirs were removed from the device. The device was sealed with epoxy for preventing evaporation during cultivation.

As soon as droplet generation was completed, the device was examined by microscopy. Pictures at the beginning and the end of cultivation were taken by Olympus BX-51 and DP-71 with 20x objective lens. The device was placed in an incubator of 30 °C for cultivation and pictures were taken as needed.

5.4.4 Retrieval of droplets after cultivation

After the cultivation, the droplets were collectively retrieved from the device for further analysis. The epoxy used for sealing was detached from the device first and a reservoir was UV-glued at the inlet for oil phase. The inlet for aqueous phase was sealed with UV glue and the outlet was left open. 20 μl of HFE-7500 without surfactant was added to the reservoir and slowly pushed using a syringe. The droplets coming out from the device was collected at the outlet using a micropipette with a 20 μl XL tip. The collected droplets were directly transferred to a bead tube (MOBio) for genomic DNA extraction or an Eppendorf tube for further cultivation.

5.4.5 16S rRNA library construction and sequencing

Genomic DNA was extracted from the culture or cell stock using MagNA Pure Compact (Roche). The sample was mixed with 150ml of bacterial lysis buffer (Roche), lysed by bead beating, treated with Proteinase K and processed by MagNA Pure Compact machine for isolation of genomic DNA. The elution volume was 50 μl . Concentration of DNA was measured using NanoDrop.

100ng of extracted metagenomic DNA was used as a template for a 25- μ l mixture of 16S rDNA PCR by Illustra PuReTaq Ready-to-Go PCR beads (GE healthcare). 8F (5'-AGA GTT TGA TCC TGG CTC AG-3') and 1492R (5'-GGT TAC CTT GTT ACG ACT T-3') universal primers were used and two replicates were prepared. Amplicon was combined, purified (Illustra MicroSpin Column, GE healthcare) and measured by NanoDrop. Right after the purification, 100ng of purified amplicon was ligated to TOPO TA vector (Invitrogen) for 30 minutes and one third of the ligation mixture was transformed into E. coli. After overnight incubation, 96 colonies were picked from a plate for planktonic culture. The inserts of 96 colonies were confirmed by PCR using M13 primers and planktonic cultures as templates. PCR products were purified by ExoSAP-IT reactions (USB) and submitted for Sanger sequencing with M13 primers to University of Michigan Sequencing Core. The sequences were analyzed using ribosomal database project website.

5.4.6 Terminal restriction fragment length polymorphism (TRFLP)

Metagenomic DNA extracted as described above was also used as a template of PCR reaction for TRFLP. Three replicates of 25- μ l reaction mixture were prepared with 70ng of genomic DNA, 6-FAM labeled universal 8F primer and non-labeled universal 1492R primer. Amplicon was combined, purified (PCR purification kit, Qiagen) and measured by NanoDrop. 300ng of purified amplicon was digested with each of MspI and RsaI for 2 hours and purified with nucleotide purification kit (Qiagen) for not losing small fragments of DNA. Digested samples were submitted to University of Michigan Sequencing Core for genotyping capillary electrophoresis.

Raw data of electrophoresis was analyzed by peak labeling of Peak Scanner v.1.0 software (ABI Biosystems). Labeled peaks were plotted by an in-house program coded in Python and MATLAB. Individual peaks was identified by comparison to the result of library sequencing.

CHAPTER VI

Concluding Remarks and Future Directions

6.1 Concluding remarks

6.1.1 Droplet-enabled co-cultivation of microbial communities

In order to expand the repertoire of cultivable species from natural microbial communities and to characterize co-cultivated communities, we have developed a microfluidic device to co-cultivate symbiotic microbial communities⁸⁹. Using aqueous micro-droplets dispersed in a continuous oil phase, the device can readily encapsulate and co-cultivate subsets of a community. A synthetic model system consisting of cross-feeding *E. coli* mutants was used to mimic compositions of symbionts and other microbes in natural microbial communities.

We have demonstrated that microfluidically generated droplets can be effectively utilized to co-cultivate microbes and detect symbiotic relationships. Two features of our microfluidic device contributed to this effectiveness. First, due to its small dimensions and rapid operation, our droplets based device can achieve compartmentalization of microbial communities in a highly parallel and automated manner. Second, the interface between the aqueous phase in the droplet and the oil phase prevents molecular exchanges, and hence the cultivation environment in individual droplets is completely localized.

We hypothesized that compartmentalization of different microbial species in a community are independent events and for each species. The experimentally measured distribution of droplets carrying various numbers of cells agreed very well with calculated values using the Poisson distribution. Therefore, the distribution of encapsulated subsets of a microbial community is highly predictable given the total cell concentration and composition of the community. Accordingly, for a given community composition, it is possible to determine the optimal cell density of the seed culture for a fixed device to achieve a desired droplet distribution.

In natural microbial communities, symbiotic partners might account for a small fraction of the total population. To mimic such conditions in nature, we further examined various compositions of *E. coli* triplet system. Our device was able to detect pair-wise symbiotic relationship when one partner accounted for as low as 1% of the total population or each symbiont was about 3% of the artificial community.

For co-cultivation and characterization of natural microbiota, further genetic analysis is required because microbes are not labeled and identified. A drug-producing natural microbiota isolated from tunicate has been co-cultivated in droplets. The droplets were collectively retrieved from devices after cultivation and analyzed by terminal restriction fragment length polymorphism (TRFLP) and 16S rRNA sequencing. TRFLP results showed that droplet-enabled co-cultivation using various culture media enriched different microbial species and they could be identified by comparison with 16S rRNA sequencing results.

6.1.2 Oxygen Gradient Construction for Co-Cultivation of Microbial Communities in Droplets

Extending the technology, we have developed a multi-layered device for co-cultivation of microbes in droplets under a gradient of oxygen concentration ranging from 0% to 21% of oxygen. Our device is composed of two glass layers with fluid channels

separated by a PDMS membrane. To demonstrate that the gas phase can penetrate Parylene-coated PDMS membrane, the oxygen concentration of droplets were monitored in real time when the gas flow was changed from pure nitrogen to oxygen. Oxygen concentration measurement was performed using ruthenium tris(2,2'-dipyridyl) dichloride hydrate (RTDP). It took about two hours to reach a new equilibrium due to Parylene film, nevertheless, the gas beneath the PDMS membrane was transferred effectively to the droplets in the liquid channel. Oxygen gradient is established and maintained via a tree-shaped channel mixing humidified nitrogen and air flows, which is then transferred through the porous PDMS membrane to the chambers in the liquid channel incubating droplets. In order to prevent the evaporation, humidification bottles half-filled with DI water are inserted between pressure regulators and gas inlets of the device. With the humidification bottles installed, the device could stably incubate droplets for at least 48 hours.

A murine fecal microbiota, which lived with limited oxygen concentration in their original environment, was cultivated and different species were enriched in chambers featuring different oxygen conditions. Combined with the localization of symbiotic microbes in droplets, establishment of oxygen conditions mimicking their natural habitats can expand the repertoire of cultivable microbes, and thus, facilitate the elucidation of microbial interactions in a community.

6.1.3 Automated sorting of droplets

To fulfill the requirement of further parallelization and automation of the droplet-enabled technology, we have developed a simple and robust device for incubation of millions of droplets for a week using a microcentrifuge tube. A Teflon tube with hydrophobic surface and the inner diameter equivalent to microfluidic channel is used to connect the incubation tube and a device. It is plugged tightly into an outlet or an inlet of a PDMS device and shear force is minimized to avoid breakup of

droplets during the transfer process. Microfluidically generated droplets can provide well-localized environment for cultivation of microbes in a highly parallel manner. Droplets are stable enough to maintain their monodispersity during incubation and transport from or to a device.

To facilitate analysis downstream of parallel droplet-enabled cultivation for various applications, we have developed a microfluidic device for automated hydrodynamic droplet sorting. The device consisted of T-junction for droplet spacing and a Y-shaped branch for droplet sorting. Automated sorting was performed hydrodynamically based on the fluorescent image analysis of droplet images representing cell density after cultivation. Two possible applications include the co-cultivation of complex natural microbial communities and screening of strain libraries for microbial engineering.

6.2 Future directions

6.2.1 Co-cultivation of natural microbial communities under oxygen gradient

Droplet-enabled co-cultivation under various oxygen concentrations can be utilized for culture-dependent research of microbial ecology to investigate microbial interactions in environments mimicking their original habitats. For example, drug-producing tunicate microbiota living in shallow sea may require microaerobic environment for their proliferation. In our research, we co-cultivated tunicate microbiota aerobically using a simple glass device. The oxygen gradient-generating device may support the growth of various microaerobes dwelling in the tunicate.

However, there still remains a challenge in isolation of endosymbiotic microbes buried in tunicate tissue while maintaining their viability. We showed that half of metagenomic DNA originated from the drug-producing bacterium, but we lost them

after an isolation process using mechanical blending. Thus, a more effective method is required for isolation of the target microbe. Although a standardized protocol to isolate endosymbionts has not been established, a few extraction buffers and homogenization methods can be explored for our tunicate microbiota^{62,22}. After the isolation of the target microbes, optimization of the culture medium will also be needed to support their growth under microaerobic environment. Since the 16S rRNA sequence of *Candidatus frumentensis* is phylogenetically close to that of *Coxiella burnetii*, information of the broth used to cultivate *C. burnetii* can be used to optimize our medium for *C. frumentensis*.⁸⁷ Cultivated droplets will be analyzed by TRFLP to confirm enrichment of the target microbe.

In addition, human microbiota of various body sites include microbes with a wide range of oxygen tolerance and preference. In particular, the human gut microbiota contains microaerobes, facultative anaerobes and obligate anaerobes^{50,64,41}. Oral³⁴, skin⁴⁵ and airway⁴² microbial communities comprise a range of microbes from aerobes to obligate anaerobes. Comparison of 16S rDNA sequences and TRFLP will identify well-grown species from each chamber. Providing various oxygen concentrations in one device by construction of gradient can greatly reduce cost and labor required for comprehensive culture-dependent investigation. Droplet-enabled co-cultivation can be applied to various natural microbiota for characterization of their innate microbial interactions. Co-cultivated droplets can be transferred to automated sorting devices and characterized after sorting.

6.2.2 Application of automated droplet sorting

We have developed a microfluidic platform for droplet incubation that can handle 10^6 droplets for automated sorting. As an initial application, the technology will be utilized for high-throughput screening of engineered *E. coli* libraries for improved isobutanol-tolerance for more efficient biofuel production. Isobutanol is a promising

biofuel with high energy density and octane value for gasoline replacement⁸. Titer of isobutanol, however, is severely limited due to its toxicity to biofuel-producing microbes. Thus, improvement of isobutanol tolerance can enhance productivity of microbial strains. Another student in Lin lab is combining adaptive evolution and genome engineering to generate a library with 10^{11} mutant strains, which will require high-throughput screening to isolate highly functional mutants.

Based on results from previous studies on isobutanol tolerance of *E. coli*, 37 genetic loci of *E. coli* have been selected for multiplex genome engineering and the parental strain was fluorescently labeled with YFP for monitoring of growth. After the library is generated, single cells from the library will be localized in droplets of isobutanol-spiked media for cultivation, and droplets carrying well-grown mutant will be screened using the automated droplet sorting device. In order to provide precise amount of isobutanol in droplets, phase partitioning of isobutanol between aqueous and oil phase will be measured by HPLC. The automated sorting will be followed by sequencing of strains retrieved from individual droplets for elucidation of key mutations associated with higher isobutanol tolerance. Utilization of microfluidics for high-throughput screening will be an efficient and cost-saving approach for microbial engineering.

Moreover, the capability of handling a large number of droplets enables the investigation of complex natural microbial communities. If a simple community consists of 4 members with identical relative abundances, about 100 droplets can cover all 16 possible combinations of the members with an average initial number of cells of 3 to 5 in a droplet. As the complexity of a community increases, the number of droplets required to generate all combinations increases dramatically. For a 15-member community, 10^5 droplets are required to generate about 33000 combinations with an average number of cells of 3 per droplet. If each member is at different level of relative abundance, which is more likely in most natural microbiota, the number of droplets should be increased even further. Therefore, co-cultivation of a natural

microbial community to distinguish symbiotic relationships requires a large number of droplets, and consequently, automated sorting. One challenge for automated sorting of a co-cultivated natural microbial community is that the image analysis should depend on reflective images, because no natural microbe is fluorescently labeled. We are currently developing a reflective image analysis module. In addition, throughput of sorting can be improved through increase of sorting rate by applying electric pulses to control droplet path instead of hydrodynamic control at Y-branch.

6.2.3 Further device development and investigation of microbial communities

6.2.3.1 Droplet FISH

In this dissertation, off-chip genetic analyses including TRFLP and 16S rDNA library sequencing were performed on co-cultivated natural microbial communities. On-chip identification will be a promising approach to render on-line integrated co-cultivation and identification. Loss of droplets during transfer of droplets from microfluidic devices to off-chip analyses platforms will be minimized. In particular, fluorescence in situ hybridization (FISH) can be utilized to identify microbial species with fluorescently labeled DNA probes¹⁰⁹, and thus, it can facilitate automated sorting. Combining co-cultivation and FISH can provide valuable information on synergistic relationships by analyzing cell clusters developed in droplets. To carry out the FISH procedure involving fixation and hybridization, microfluidic components for droplet splitting, droplet merging¹⁶ or reagent injection¹ will need to be added to inject chemicals and probes after the cultivation step.

Addition of on-chip FISH will be especially useful if there are one or two target species of interest in a community. For example, implementation of FISH will greatly facilitate the investigation of drug-producing *C. frumentensis* in the tunicate microbial community. Without droplet FISH, every droplet would need to be retrieved and

analyzed to determine if the target microbe was enriched. Fluorescent labeling of the target microbe facilitates detection and sorting of the droplets carrying the target microbes, and therefore, greatly saves cost, time and labor. In addition, FISH analysis can reveal whether or not the bacteria forms a biofilm or the symbiotic relationship requires physical contacts between different species. By fixing and labeling cells without lysis, we can maintain microbes in their original morphology and distance among neighbors.

Moreover, combining the usage of a large number of droplets for co-cultivating various subsets of a complex natural microbial community and appropriate labeling of specific microbial species using FISH, we will be able to reveal antagonistic relationships between members as well as synergistic relationships which this dissertation has mainly discussed. If a target species is suppressed in specific droplets, analyzing those droplets will show which community members inhibit the growth of the target bacterium. Elucidation of such microbial interactions might have important implications for many applications such as the diagnosis and treatment of polymicrobial diseases.

6.2.3.2 Metagenomic investigation

Droplet-driven mixed cultures can be further studied using a variety of characterization methods such as metagenome sequencing. Simple identification can provide information about which species can grow well together, but doesn't elucidate why they are beneficial to each other at molecular level. Whole genome amplification followed by metagenome sequencing will potentially lead to comprehensive and detailed understanding of the genetic basis underlying the microbial interactions^{67,107}. Computational metagenomic tools can be employed to analyze the large volume of data generated from metagenomic sequencing. Such analysis will reveal molecular mechanisms underlying the microbial interactions, for examples, which metabolic functions

a species lacks or supports neighbors with.

BIBLIOGRAPHY

BIBLIOGRAPHY

1. Abate, A. R., T. Hung, P. Mary, J. J. Agresti, and D. A. Weitz (2010), High-throughput injection with microfluidics using picoinjectors, *Proc Natl Acad Sci U S A*, *107*(45), 19,163–6, doi:10.1073/pnas.1006888107.
2. Adler, M., M. Polinkovsky, E. Gutierrez, and A. Groisman (2010), Generation of oxygen gradients with arbitrary shapes in a microfluidic device, *Lab Chip*, *10*(3), 388–91, doi:10.1039/b920401f.
3. Agresti, J. J., et al. (2010), Ultrahigh-throughput screening in drop-based microfluidics for directed evolution, *Proc Natl Acad Sci U S A*, *107*(9), 4004–9, doi:10.1073/pnas.0910781107.
4. Ahn, K., C. Kerbage, T. Hunt, R. Westervelt, D. Link, and D. Weitz (2006), Dielectrophoretic manipulation of drops for high-speed microfluidic sorting devices, *APPLIED PHYSICS LETTERS*, *88*(2), doi:10.1063/1.2164911.
5. Alain, K., and J. Querellou (2009), Cultivating the uncultured: limits, advances and future challenges, *Extremophiles*, *13*(4), 583–94, doi:10.1007/s00792-009-0261-3.
6. Amin, S. A., D. H. Green, M. C. Hart, F. C. Küpper, W. G. Sunda, and C. J. Carrano (2009), Photolysis of iron–siderophore chelates promotes bacterial–algal mutualism, *Proceedings of the National Academy of Sciences*, *106*(40), 17,071–17,076, doi:10.1073/pnas.0905512106.
7. Atencia, J., J. Morrow, and L. E. Locascio (2009), The microfluidic palette: a diffusive gradient generator with spatio-temporal control, *Lab Chip*, *9*(18), 2707–14, doi:10.1039/b902113b.
8. Atsumi, S., and J. C. Liao (2008), Metabolic engineering for advanced biofuels production from escherichia coli, *Curr Opin Biotechnol*, *19*(5), 414–9, doi:10.1016/j.copbio.2008.08.008.
9. Azam, F., and F. Malfatti (2007), Microbial structuring of marine ecosystems, *Nat Rev Microbiol*, *5*(10), 782–91, doi:10.1038/nrmicro1747.
10. Baldrian, P., I. M. Head, J. I. Prosser, M. Schloter, K. Smalla, and C. C. Tebbe (2011), Ecology and metagenomics of soil microorganisms, *FEMS Microbiol Ecol*, *78*(1), 1–2, doi:10.1111/j.1574-6941.2011.01184.x.

11. Baret, J.-C. (2012), Surfactants in droplet-based microfluidics, *Lab Chip*, *12*, 422–433, doi:10.1039/C1LC20582J.
12. Baret, J.-C., et al. (2009), Fluorescence-activated droplet sorting (fads): efficient microfluidic cell sorting based on enzymatic activity, *Lab Chip*, *9*(13), 1850–8, doi:10.1039/b902504a.
13. Belenguer, A., S. H. Duncan, A. G. Calder, G. Holtrop, P. Louis, G. E. Lobley, and H. J. Flint (2006), Two routes of metabolic cross-feeding between bifidobacterium adolescentis and butyrate-producing anaerobes from the human gut, *Appl Environ Microbiol*, *72*(5), 3593–9, doi:10.1128/AEM.72.5.3593-3599.2006.
14. Boedicker, J. Q., M. E. Vincent, and R. F. Ismagilov (2009), Microfluidic confinement of single cells of bacteria in small volumes initiates high-density behavior of quorum sensing and growth and reveals its variability, *Angew Chem Int Ed Engl*, *48*(32), 5908–11, doi:10.1002/anie.200901550.
15. Bollmann, A., K. Lewis, and S. S. Epstein (2007), Incubation of environmental samples in a diffusion chamber increases the diversity of recovered isolates, *Appl Environ Microbiol*, *73*(20), 6386–90, doi:10.1128/AEM.01309-07.
16. Brouzes, E., et al. (2009), Droplet microfluidic technology for single-cell high-throughput screening, *Proceedings of the National Academy of Sciences*, doi:10.1073/pnas.0903542106.
17. Bruns, A., U. Nübel, H. Cypionka, and J. Overmann (2003), Effect of signal compounds and incubation conditions on the culturability of freshwater bacterioplankton, *Applied and Environmental Microbiology*, *69*(4), 1980–1989, doi:10.1128/AEM.69.4.1980-1989.2003.
18. Buckley, D. H., and T. M. Schmidt (2003), Diversity and dynamics of microbial communities in soils from agro-ecosystems, *Environmental Microbiology*, *5*(6), 441–452, doi:10.1046/j.1462-2920.2003.00404.x.
19. Chabert, M., and J.-L. Viovy (2008), Microfluidic high-throughput encapsulation and hydrodynamic self-sorting of single cells, *Proceedings of the National Academy of Sciences*, *105*(9), 3191–3196, doi:10.1073/pnas.0708321105.
20. Chen, Y.-A., A. D. King, H.-C. Shih, C.-C. Peng, C.-Y. Wu, W.-H. Liao, and Y.-C. Tung (2011), Generation of oxygen gradients in microfluidic devices for cell culture using spatially confined chemical reactions, *Lab Chip*, *11*(21), 3626–33, doi:10.1039/c1lc20325h.
21. Clausell-Tormos, J., et al. (2008), Droplet-based microfluidic platforms for the encapsulation and screening of mammalian cells and multicellular organisms, *Chem Biol*, *15*(5), 427–37, doi:10.1016/j.chembiol.2008.04.004.

22. Cockrell, D. C., P. A. Beare, E. R. Fischer, D. Howe, and R. A. Heinzen (2008), A method for purifying obligate intracellular coxiella burnetii that employs digitonin lysis of host cells, *J Microbiol Methods*, *72*(3), 321–5, doi:10.1016/j.mimet.2007.12.015.
23. Cogen, A. L., V. Nizet, and R. L. Gallo (2008), Skin microbiota: a source of disease or defence?, *Br J Dermatol*, *158*(3), 442–55, doi:10.1111/j.1365-2133.2008.08437.x.
24. Connon, S. A., and S. J. Giovannoni (2002), High-throughput methods for culturing microorganisms in very-low-nutrient media yield diverse new marine isolates, *Applied and Environmental Microbiology*, *68*(8), 3878–3885, doi:10.1128/AEM.68.8.3878-3885.2002.
25. Costello, E. K., C. L. Lauber, M. Hamady, N. Fierer, J. I. Gordon, and R. Knight (2009), Bacterial community variation in human body habitats across space and time, *Science*, *326*(5960), 1694–7, doi:10.1126/science.1177486.
26. Cuevas, C., et al. (2000), Synthesis of ecteinascidin et-743 and phthalascidin pt-650 from cyanosafraicin b, *Organic Letters*, *2*(16), 2545–2548, doi:10.1021/ol0062502.
27. Daniel, R. (2005), The metagenomics of soil, *Nat Rev Microbiol*, *3*(6), 470–8, doi:10.1038/nrmicro1160.
28. Davis, K. E. R., S. J. Joseph, and P. H. Janssen (2005), Effects of growth medium, inoculum size, and incubation time on culturability and isolation of soil bacteria, *Appl Environ Microbiol*, *71*(2), 826–34, doi:10.1128/AEM.71.2.826-834.2005.
29. DeLong, E. F. (2005), Microbial community genomics in the ocean, *Nat Rev Microbiol*, *3*(6), 459–69, doi:10.1038/nrmicro1158.
30. DeLong, E. F. (2009), The microbial ocean from genomes to biomes, *Nature*, *459*(7244), 200–6, doi:10.1038/nature08059.
31. Denou, E., E. Rezzonico, J.-M. Panoff, F. Arigoni, and H. Bruessow (2009), A mesocosm of lactobacillus johnsonii, bifidobacterium longum, and escherichia coli in the mouse gut, *DNA AND CELL BIOLOGY*, *28*(8), 413–422, doi:10.1089/dna.2009.0873, aSM Beneficial Microbes Conference, San Diego, CA, OCT, 2008.
32. Dertinger, S. K. W., D. T. Chiu, N. L. Jeon, and G. M. Whitesides (2001), Generation of gradients having complex shapes using microfluidic networks, *Analytical Chemistry*, *73*(6), 1240–1246, doi:10.1021/ac001132d.
33. Dethlefsen, L., M. McFall-Ngai, and D. A. Relman (2007), An ecological and evolutionary perspective on human-microbe mutualism and disease, *Nature*, *449*(7164), 811–8, doi:10.1038/nature06245.

34. Dewhurst, F. E., T. Chen, J. Izard, B. J. Paster, A. C. R. Tanner, W.-H. Yu, A. Lakshmanan, and W. G. Wade (2010), The human oral microbiome, *J Bacteriol*, *192*(19), 5002–17, doi:10.1128/JB.00542-10.
35. Dietrich, J. A., A. E. McKee, and J. D. Keasling (2010), High-throughput metabolic engineering: Advances in small-molecule screening and selection, in *ANNUAL REVIEW OF BIOCHEMISTRY, VOL 79, Annual Review of Biochemistry*, vol. 79, edited by R. Kornberg, C. Raetz, J. Rothman, and J. Thorner, pp. 563–590, doi:10.1146/annurev-biochem-062608-095938.
36. D’Onofrio, A., J. M. Crawford, E. J. Stewart, K. Witt, E. Gavrish, S. Epstein, J. Clardy, and K. Lewis (2010), Siderophores from neighboring organisms promote the growth of uncultured bacteria, *Chem Biol*, *17*(3), 254–64, doi:10.1016/j.chembiol.2010.02.010.
37. Elowitz, M. B., A. J. Levine, E. D. Siggia, and P. S. Swain (2002), Stochastic gene expression in a single cell, *Science*, *297*(5584), 1183–6, doi:10.1126/science.1070919.
38. Englert, D. L., M. D. Manson, and A. Jayaraman (2009), Flow-based microfluidic device for quantifying bacterial chemotaxis in stable, competing gradients, *Appl Environ Microbiol*, *75*(13), 4557–64, doi:10.1128/AEM.02952-08.
39. Ferrari, B. C., S. J. Binnerup, and M. Gillings (2005), Microcolony cultivation on a soil substrate membrane system selects for previously uncultured soil bacteria, *Appl Environ Microbiol*, *71*(12), 8714–20, doi:10.1128/AEM.71.12.8714-8720.2005.
40. Ferrari, B. C., T. Winsley, M. Gillings, and S. Binnerup (2008), Cultivating previously uncultured soil bacteria using a soil substrate membrane system, *Nat Protoc*, *3*(8), 1261–9, doi:10.1038/nprot.2008.102.
41. FOX, J., F. DEWHIRST, J. TULLY, B. PASTER, L. YAN, N. TAYLOR, M. COLLINS, P. GORELICK, and J. WARD (1994), *Helicobacter hepaticus* sp-nov, a microaerophilic bacterium isolated from livers and intestinal mucosal scrapings from mice, *JOURNAL OF CLINICAL MICROBIOLOGY*, *32*(5), 1238–1245.
42. Frank, D. N., L. M. Feazel, M. T. Bessesen, C. S. Price, E. N. Janoff, and N. R. Pace (2010), The human nasal microbiota and staphylococcus aureus carriage, *PLoS One*, *5*(5), e10,598, doi:10.1371/journal.pone.0010598.
43. Fuqua, C., and E. P. Greenberg (2002), Listening in on bacteria: acyl-homoserine lactone signalling, *Nat Rev Mol Cell Biol*, *3*(9), 685–95, doi:10.1038/nrm907.
44. Gill, S. R., et al. (2006), Metagenomic analysis of the human distal gut microbiome, *Science*, *312*(5778), 1355–9, doi:10.1126/science.1124234.

45. Grice, E. A., et al. (2008), A diversity profile of the human skin microbiota, *Genome Res*, *18*(7), 1043–50, doi:10.1101/gr.075549.107.
46. Grice, E. A., et al. (2009), Topographical and temporal diversity of the human skin microbiome, *Science*, *324*(5931), 1190–2, doi:10.1126/science.1171700.
47. Grodrian, A., J. Metze, T. Henkel, K. Martin, M. Roth, and J. M. Köhler (2004), Segmented flow generation by chip reactors for highly parallelized cell cultivation, *Biosens Bioelectron*, *19*(11), 1421–8, doi:10.1016/j.bios.2003.12.021.
48. Guarner, F., and J.-R. Malagelada (2003), Gut flora in health and disease, *Lancet*, *361*(9356), 512–9, doi:10.1016/S0140-6736(03)12489-0.
49. Harris, J. (2009), Soil microbial communities and restoration ecology: facilitators or followers?, *Science*, *325*(5940), 573–4, doi:10.1126/science.1172975.
50. Hartman, A. L., D. M. Lough, D. K. Barupal, O. Fiehn, T. Fishbein, M. Zasloff, and J. A. Eisen (2009), Human gut microbiome adopts an alternative state following small bowel transplantation, *Proceedings of the National Academy of Sciences*, doi:10.1073/pnas.0904847106.
51. Hayashi, A., H. Aoyagi, T. Yoshimura, and H. Tanaka (2007), Development of novel method for screening microorganisms using symbiotic association between insect (*Coptotermes formosanus shiraki*) and intestinal microorganisms, *J Biosci Bioeng*, *103*(4), 358–67, doi:10.1263/jbb.103.358.
52. Holtze, C., et al. (2008), Biocompatible surfactants for water-in-fluorocarbon emulsions, *Lab Chip*, *8*(10), 1632–9, doi:10.1039/b806706f.
53. Hong, S.-H., J. Bunge, S.-O. Jeon, and S. S. Epstein (2006), Predicting microbial species richness, *Proceedings of the National Academy of Sciences of the United States of America*, *103*(1), 117–122, doi:10.1073/pnas.0507245102.
54. Hongoh, Y., et al. (2008), Complete genome of the uncultured termite group 1 bacteria in a single host protist cell, *Proceedings of the National Academy of Sciences*, *105*(14), 5555–5560, doi:10.1073/pnas.0801389105.
55. Huber, J. A., D. B. Mark Welch, H. G. Morrison, S. M. Huse, P. R. Neal, D. A. Butterfield, and M. L. Sogin (2007), Microbial population structures in the deep marine biosphere, *Science*, *318*(5847), 97–100, doi:10.1126/science.1146689.
56. Hugenholtz, P., B. Goebel, and N. Pace (1998), Impact of culture-independent studies on the emerging phylogenetic view of bacterial diversity, *JOURNAL OF BACTERIOLOGY*, *180*(18), 4765–4774.
57. Imlay, J. (2002), How oxygen damages microbes: Oxygen tolerance and obligate anaerobiosis, in *ADVANCES IN MICROBIAL PHYSIOLOGY, VOL 46, ADVANCES IN MICROBIAL PHYSIOLOGY*, vol. 46, pp. 111–153, doi:10.1016/S0065-2911(02)46003-1.

58. Ingham, C. J., A. Sprenkels, J. Bomer, D. Molenaar, A. van den Berg, J. E. T. van Hylckama Vlieg, and W. M. de Vos (2007), The micro-petri dish, a million-well growth chip for the culture and high-throughput screening of microorganisms, *Proceedings of the National Academy of Sciences*, *104*(46), 18,217–18,222, doi:10.1073/pnas.0701693104.
59. Inoue, I., Y. Wakamoto, H. Moriguchi, K. Okano, and K. Yasuda (2001), On-chip culture system for observation of isolated individual cells, *Lab Chip*, *1*(1), 50–5, doi:10.1039/b103931h.
60. Irimia, D., D. A. Geba, and M. Toner (2006), Universal microfluidic gradient generator, *Analytical Chemistry*, *78*(10), 3472–3477, doi:10.1021/ac0518710.
61. Janda, J. M., and S. L. Abbott (2007), 16s rRNA gene sequencing for bacterial identification in the diagnostic laboratory: pluses, perils, and pitfalls, *J Clin Microbiol*, *45*(9), 2761–4, doi:10.1128/JCM.01228-07.
62. Jargeat, P., C. Cosseau, B. Ola'h, A. Jauneau, P. Bonfante, J. Batut, and G. Bécard (2004), Isolation, free-living capacities, and genome structure of "candidatus glomeribacter gigasporarum," the endocellular bacterium of the mycorrhizal fungus *gigaspora margarita*, *J Bacteriol*, *186*(20), 6876–84, doi:10.1128/JB.186.20.6876-6884.2004.
63. Jeon, N. L., S. K. W. Dertinger, D. T. Chiu, I. S. Choi, A. D. Stroock, and G. M. Whitesides (2000), Generation of solution and surface gradients using microfluidic systems, *Langmuir*, *16*(22), 8311–8316, doi:10.1021/la000600b.
64. John, A., P. L. Connerton, N. Cummings, and I. F. Connerton (2011), Profound differences in the transcriptome of *Campylobacter jejuni* grown in two different, widely used, microaerobic atmospheres, *Res Microbiol*, *162*(4), 410–8, doi:10.1016/j.resmic.2011.02.004.
65. Jullien, M. C., M. J. T. M. Ching, C. Cohen, L. Menetrier, and P. Tabeling (2009), Droplet breakup in microfluidic T-junctions at small capillary numbers, *PHYSICS OF FLUIDS*, *21*(7), doi:10.1063/1.3170983.
66. Kaeberlein, T., K. Lewis, and S. S. Epstein (2002), Isolating "uncultivable" microorganisms in pure culture in a simulated natural environment, *Science*, *296*(5570), 1127–9, doi:10.1126/science.1070633.
67. Kalyuzhnaya, M. G., et al. (2008), High-resolution metagenomics targets specific functional types in complex microbial communities, *Nat Biotechnol*, *26*(9), 1029–34, doi:10.1038/nbt.1488.
68. Kim, S., H. J. Kim, and N. L. Jeon (2010), Biological applications of microfluidic gradient devices, *Integr Biol (Camb)*, *2*(11-12), 584–603, doi:10.1039/c0ib00055h.

69. Köster, S., et al. (2008), Drop-based microfluidic devices for encapsulation of single cells, *Lab Chip*, 8(7), 1110–5, doi:10.1039/b802941e.
70. Lam, R. H. W., M.-C. Kim, and T. Thorsen (2009), Culturing aerobic and anaerobic bacteria and mammalian cells with a microfluidic differential oxygenator, *Analytical Chemistry*, 81(14), 5918–5924, doi:10.1021/ac9006864, PMID: 19601655.
71. Li, M., et al. (2008), Symbiotic gut microbes modulate human metabolic phenotypes, *Proceedings of the National Academy of Sciences*, 105(6), 2117–2122, doi:10.1073/pnas.0712038105.
72. Lin, F., W. Saadi, S. W. Rhee, S.-J. Wang, S. Mittal, and N. L. Jeon (2004), Generation of dynamic temporal and spatial concentration gradients using microfluidic devices, *Lab Chip*, 4(3), 164–7, doi:10.1039/b313600k.
73. Liu, W., H. J. Kim, E. M. Lucchetta, W. Du, and R. F. Ismagilov (2009), Isolation, incubation, and parallel functional testing and identification by fish of rare microbial single-copy cells from multi-species mixtures using the combination of chemistride and stochastic confinement, *Lab Chip*, 9(15), 2153–62, doi:10.1039/b904958d.
74. Liu, W. T., T. L. Marsh, H. Cheng, and L. J. Forney (1997), Characterization of microbial diversity by determining terminal restriction fragment length polymorphisms of genes encoding 16s rRNA., *Applied and Environmental Microbiology*, 63(11), 4516–22.
75. Marcy, Y., et al. (2007), Dissecting biological “dark matter” with single-cell genetic analysis of rare and uncultivated tm7 microbes from the human mouth, *Proceedings of the National Academy of Sciences*, 104(29), 11,889–11,894, doi: 10.1073/pnas.0704662104.
76. Martin, F.-P. J., et al. (2008), Probiotic modulation of symbiotic gut microbial-host metabolic interactions in a humanized microbiome mouse model, *Mol Syst Biol*, 4, 157, doi:10.1038/msb4100190.
77. Martin, K., T. Henkel, V. Baier, A. Grodrian, T. Schön, M. Roth, J. Michael Köhler, and J. Metze (2003), Generation of larger numbers of separated microbial populations by cultivation in segmented-flow microdevices, *Lab Chip*, 3(3), 202–7, doi:10.1039/b301258c.
78. Mazmanian, S. K., J. L. Round, and D. L. Kasper (2008), A microbial symbiosis factor prevents intestinal inflammatory disease, *Nature*, 453(7195), 620–5, doi: 10.1038/nature07008.
79. Mehta, G., et al. (2007), Quantitative measurement and control of oxygen levels in microfluidic poly(dimethylsiloxane) bioreactors during cell culture, *Biomed Microdevices*, 9(2), 123–34, doi:10.1007/s10544-006-9005-7.

80. Merkel, T. C., V. I. Bondar, K. Nagai, B. D. Freeman, and I. Pinnau (2000), Gas sorption, diffusion, and permeation in poly(dimethylsiloxane), *Journal of Polymer Science Part B: Polymer Physics*, *38*(3), 415–434, doi:10.1002/(SICI)1099-0488(20000201)38:3<415::AID-POLB8>3.0.CO;2-Z.
81. Moss, C., D. H. Green, B. Pérez, A. Velasco, R. Henríquez, and J. D. McKenzie (2003), Intracellular bacteria associated with the ascidian <i>ecteinascidia turbinata</i>: phylogenetic and in situ hybridisation analysis, *Marine Biology*, *143*, 99–110, 10.1007/s00227-003-1060-5.
82. Nell, S., S. Suerbaum, and C. Josenhans (2010), The impact of the microbiota on the pathogenesis of ibd: lessons from mouse infection models, *Nat Rev Microbiol*, *8*(8), 564–77, doi:10.1038/nrmicro2403.
83. Nichols, D. (2007), Cultivation gives context to the microbial ecologist, *FEMS Microbiol Ecol*, *60*(3), 351–7, doi:10.1111/j.1574-6941.2007.00332.x.
84. Nichols, D., et al. (2008), Short peptide induces an "uncultivable" microorganism to grow in vitro, *Appl Environ Microbiol*, *74*(15), 4889–97, doi:10.1128/AEM.00393-08.
85. Niu, X., M. Zhang, S. Peng, W. Wen, and P. Sheng (2007), Real-time detection, control, and sorting of microfluidic droplets, *Biomicrofluidics*, *1*(4), 44,101, doi:10.1063/1.2795392.
86. Olsen, G. J., D. J. Lane, S. J. Giovannoni, N. R. Pace, and D. A. Stahl (1986), Microbial ecology and evolution: A ribosomal rna approach, *Annual Review of Microbiology*, *40*(1), 337–365, doi:10.1146/annurev.mi.40.100186.002005.
87. Omsland, A., D. C. Cockrell, D. Howe, E. R. Fischer, K. Virtaneva, D. E. Sturdevant, S. F. Porcella, and R. A. Heinzen (2009), Host cell-free growth of the q fever bacterium *coxiella burnetii*, *Proceedings of the National Academy of Sciences*, *106*(11), 4430–4434, doi:10.1073/pnas.0812074106.
88. Parales, R. E., N. C. Bruce, A. Schmid, and L. P. Wackett (2002), Biodegradation, biotransformation, and biocatalysis (b3), *Applied and Environmental Microbiology*, *68*(10), 4699–4709, doi:10.1128/AEM.68.10.4699-4709.2002.
89. Park, J., A. Kerner, M. A. Burns, and X. N. Lin (2011), Microdroplet-enabled highly parallel co-cultivation of microbial communities, *PLoS One*, *6*(2), e17,019, doi:10.1371/journal.pone.0017019.
90. Pérez-Matos, A. E., W. Rosado, and N. S. Govind (2007), Bacterial diversity associated with the caribbean tunicate *ecteinascidia turbinata*, *Antonie Van Leeuwenhoek*, *92*(2), 155–64, doi:10.1007/s10482-007-9143-9.
91. Proksch, P., R. A. Edrada, and R. Ebel (2002), Drugs from the seas - current status and microbiological implications, *Appl Microbiol Biotechnol*, *59*(2-3), 125–34, doi:10.1007/s00253-002-1006-8.

92. Pull, S. L., J. M. Doherty, J. C. Mills, J. I. Gordon, and T. S. Stappenbeck (2005), Activated macrophages are an adaptive element of the colonic epithelial progenitor niche necessary for regenerative responses to injury, *Proceedings of the National Academy of Sciences of the United States of America*, *102*(1), 99–104, doi:10.1073/pnas.0405979102.
93. Rath, C. M., et al. (2011), Meta-omic characterization of the marine invertebrate microbial consortium that produces the chemotherapeutic natural product et-743, *ACS Chemical Biology*, *6*(11), 1244–1256, doi:10.1021/cb200244t.
94. Rinehart, K. L. (2000), Antitumor compounds from tunicates, *Medicinal Research Reviews*, *20*(1), 1–27, doi:10.1002/(SICI)1098-1128(200001)20:1;1::AID-MED1j3.0.CO;2-A.
95. Rinehart, K. L., T. G. Holt, N. L. Fregeau, J. G. Stroh, P. A. Keifer, F. Sun, L. H. Li, and D. G. Martin (1990), Ecteinascidins 729, 743, 745, 759a, 759b, and 770: potent antitumor agents from the caribbean tunicate ecteinascidia turbinata, *The Journal of Organic Chemistry*, *55*(15), 4512–4515, doi:10.1021/jo00302a007.
96. Rolfe, R. D., D. J. Hentges, B. J. Campbell, and J. T. Barrett (1978), Factors related to the oxygen tolerance of anaerobic bacteria, *Applied and Environmental Microbiology*, *36*(2), 306–313.
97. Sayers, E. W., et al. (2011), Database resources of the national center for biotechnology information, *Nucleic Acids Res*, *39*(Database issue), D38–51, doi:10.1093/nar/gkq1172.
98. Schink, B. (2002), Synergistic interactions in the microbial world, *Antonie van Leeuwenhoek*, *81*, 257–261, 10.1023/A:1020579004534.
99. Singh, S., S. H. Kang, A. Mulchandani, and W. Chen (2008), Bioremediation: environmental clean-up through pathway engineering, *Curr Opin Biotechnol*, *19*(5), 437–44, doi:10.1016/j.copbio.2008.07.012.
100. Skolimowski, M., M. W. Nielsen, J. Emnéus, S. Molin, R. Taboryski, C. Sternberg, M. Dufva, and O. Geschke (2010), Microfluidic dissolved oxygen gradient generator biochip as a useful tool in bacterial biofilm studies, *Lab Chip*, *10*(16), 2162–9, doi:10.1039/c003558k.
101. Stevenson, B. S., S. A. Eichorst, J. T. Wertz, T. M. Schmidt, and J. A. Breznak (2004), New strategies for cultivation and detection of previously uncultured microbes, *Appl Environ Microbiol*, *70*(8), 4748–55, doi:10.1128/AEM.70.8.4748-4755.2004.
102. Straight, P. D., and R. Kolter (2009), Interspecies chemical communication in bacterial development, *Annu Rev Microbiol*, *63*, 99–118, doi:10.1146/annurev.micro.091208.073248.

103. Strom, S. L. (2008), Microbial ecology of ocean biogeochemistry: a community perspective, *Science*, *320*(5879), 1043–5, doi:10.1126/science.1153527.
104. Tan, Y.-C., Y. Ho, and A. Lee (2008), Microfluidic sorting of droplets by size, *Microfluidics and Nanofluidics*, *4*, 343–348, 10.1007/s10404-007-0184-1.
105. Turnbaugh, P. J., R. E. Ley, M. A. Mahowald, V. Magrini, E. R. Mardis, and J. I. Gordon (2006), An obesity-associated gut microbiome with increased capacity for energy harvest, *Nature*, *444*(7122), 1027–31, doi:10.1038/nature05414.
106. Turnbaugh, P. J., R. E. Ley, M. Hamady, C. M. Fraser-Liggett, R. Knight, and J. I. Gordon (2007), The human microbiome project, *Nature*, *449*(7164), 804–10, doi:10.1038/nature06244.
107. Tyson, G. W., et al. (2004), Community structure and metabolism through reconstruction of microbial genomes from the environment, *Nature*, *428*(6978), 37–43.
108. Van Der Heijden, M. G. A., R. D. Bardgett, and N. M. Van Straalen (2008), The unseen majority: soil microbes as drivers of plant diversity and productivity in terrestrial ecosystems, *Ecology Letters*, *11*(3), 296–310, doi:10.1111/j.1461-0248.2007.01139.x.
109. Wagner, M., and S. Haider (2011), New trends in fluorescence in situ hybridization for identification and functional analyses of microbes, *Curr Opin Biotechnol*, doi:10.1016/j.copbio.2011.10.010.
110. Wang, H.-X., Z.-L. Geng, Y. Zeng, and Y.-M. Shen (2008), Enriching plant microbiota for a metagenomic library construction, *Environ Microbiol*, *10*(10), 2684–91, doi:10.1111/j.1462-2920.2008.01689.x.
111. Warnecke, F., et al. (2007), Metagenomic and functional analysis of hindgut microbiota of a wood-feeding higher termite, *Nature*, *450*(7169), 560–5, doi: 10.1038/nature06269.
112. Waters, C. M., and B. L. Bassler (2005), Quorum sensing: cell-to-cell communication in bacteria, *Annu Rev Cell Dev Biol*, *21*, 319–46, doi: 10.1146/annurev.cellbio.21.012704.131001.
113. Yeh, Y.-S., W. J. James, and H. Yasuda (1990), Polymerization of para-xylylene derivatives. vi. morphology of parylene n and parylene c films investigated by gas transport characteristics, *Journal of Polymer Science Part B: Polymer Physics*, *28*(4), 545–568, doi:10.1002/polb.1990.090280409.
114. Zengler, K., G. Toledo, M. Rappé, J. Elkins, E. J. Mathur, J. M. Short, and M. Keller (2002), Cultivating the uncultured, *Proceedings of the National Academy of Sciences*, *99*(24), 15,681–15,686, doi:10.1073/pnas.252630999.